

MALIGN: Explainable Static Raw-byte Based Malware Family Classification using Sequence Alignment

Shoumik Saha^{a,b,*}, Sadia Afroz^{c,d}, Atif Hasan Rahman^{b,*}

^aUniversity of Maryland, College Park, Maryland, United States

^bBangladesh University of Engineering and Technology (BUET), Dhaka, Bangladesh

^cICSI, University of California, Berkeley, United States

^dAvast, United States

Abstract

For a long time, malware classification and analysis have been an arms-race between antivirus systems and malware authors. Though static analysis is vulnerable to evasion techniques, it is still popular as the first line of defense in antivirus systems. But most of the static analyzers failed to gain the trust of practitioners due to their black-box nature. We propose MALIGN, a novel static malware family classification approach inspired by genome sequence alignment that can not only classify malware families but can also provide explanations for its decision. MALIGN encodes raw bytes using nucleotides and adopts genome sequence alignment approaches to create a signature of a malware family based on the conserved code segments in that family, without any human labor or expertise. We evaluate MALIGN on two malware datasets, and it outperforms other state-of-the-art machine learning-based malware classifiers (by 4.49%~0.07%), especially on small datasets (by 19.48%~1.2%). Furthermore, we explain the generated signatures by MALIGN on different malware families illustrating the kinds of insights it can provide to analysts, and show its efficacy as an analysis tool. Additionally, we evaluate its theoretical and empirical robustness against some common attacks. In this paper, we approach static malware analysis from a unique perspective, aiming to strike a delicate balance among performance, interpretability, and robustness.

Keywords: malware, sequence alignment, explainability, machine learning, adversarial

1. Introduction

Over the past decade, malware has been growing and spreading exponentially. For example, the AV-Test institute registers more than 450K new malware and potentially unwanted programs (PUP) every day (AV-Test, 2023). They found 16 million new malware in just the first 3 months of 2023.¹

To detect this rising number of malware at scale, static analysis is used as the first line of defense by all commercial antivirus (AV) systems, because it requires less computational power and time than dynamic analysis. However, dynamic analysis allows security analysts to perform more in-depth analysis by executing the malware in a sandbox or cloud, and capturing its behavior and activity (Or-Meir et al., 2019; Anderson et al., 2011; Avllazagaj et al., 2021). Additionally, static analysis is comparatively easier to evade than dynamic ones.

Like all other fields, machine learning (ML) is getting adapted to security too, including malware detection and family classification (Schultz et al., 2000; Nataraj et al., 2011; Pascanu et al., 2015; Kalash et al., 2018; Shahzad et al., 2011; Lu, 2019; Yan et al., 2018; Ahmadi et al., 2016; Raff et al., 2018).

ML has proved helpful in detecting the rising number of malware at scale. In fact, most commercial malware detectors use machine learning for their static analysis nowadays. However, these deep-learning based black-box models lack *interpretability*, and conventional explanation methods for machine learning (Zhang et al., 2019) are not suitable in security (Guo et al., 2018a). Consequently, security practitioners cannot fully trust these models, especially in safety-critical applications where the ability to explain a classification error is crucial.

Unfortunately, while a large body of work has gone into designing highly accurate static malware classifiers by outperforming each other over the past few years, very little work has been done considering the *explainability* aspect. Existing works (Arp et al., 2014; Kinkead et al., 2021; Melis et al., 2018; Liu et al., 2022; Kumar et al., 2018) on explainable malware classifier are done on extracted features, e.g., requested and used permissions, API calls, network addresses, etc., rather than analyzing the executable code directly. Thus, they can only provide explainability at a higher-level semantics, while the potential insights and new knowledge that could be extracted from low-level input features remain unexplored. This untapped information could include valuable findings such as common practices among malware authors, prevalent obfuscation techniques, and other critical insights essential for analysts.

Another shortcoming of current static malware classifiers is that they are *vulnerable* to different adversarial attacks (Song

*Corresponding authors

Email addresses: smksaha@umd.edu (Shoumik Saha), atif@cse.buet.ac.bd (Atif Hasan Rahman)

¹<https://portal.av-atlas.org/malware>

et al., 2020; Suciu et al., 2019; Demetrio et al., 2021; Ceschin et al., 2019; Kolosnjaji et al., 2018; Huang et al., 2018; Kreuk et al., 2018a). Though these adversarial attacks use different techniques and work in different settings, fundamentally, they fall under one umbrella – adding or modifying bytes (from benign files or generated using gradient approaches) without altering the malware semantics. Consequently, there have been works on proposing defenses for such attacks, e.g., monotonic classifier (Fleshman et al., 2018a), adversarial training (Lucas et al., 2023), etc.. Unfortunately, most of these defenses suffer from low standard accuracy and can provide robustness to a limited number of attacks; which introduces a trade-off between robustness and accuracy.

Moreover, end-to-end deep-learning based models are *data hungry* (Marcus, 2018). The more data they get, the better they learn the features. However, this data hunger poses a concerning challenge in the context of malware family classification, particularly in the detection of a new variant. When a new malware variant or family emerges, it takes time for AV vendors to collect enough samples from the wild. Unfortunately, the prevalence of such new variants is on a steady rise. For example, in 2020, there was a 62% rise in detected malware variants². In March 2022, there was a new record of discovering 60,000 new malware variants³. As a result, these deep-learning based approaches fail to perform at their fullest for such new malware variants due to their insufficient training set size.

All of these issues raise a crucial research question:

"Can we design a novel static analysis technique that can effectively mitigate the shortcomings (non-interpretability, vulnerability, data-hungry) mentioned above?"

In this study, we focus on a raw-byte-based static malware family classification technique as a potential answer to this question. By exploring this approach, we aim to enhance the explainability and robustness of static analysis in combating the ever-evolving landscape of malware threats.

Our Design. We propose MALIGN, a novel static malware family detection method that operates directly on the raw bytes from executables. Unlike conventional static analyzers, our approach leverages the sequence alignment mechanism from bioinformatics and incorporates it with a machine learning model. The rationale behind adopting such an alignment mechanism is the indistinct similarity between genome sequences and malware executables. Genomes contain critical regions for the survival of the organism, such as protein-coding genes where mutations (or changes in genes) can be lethal. Similarly, malware families contain malicious code blocks associated with the malicious functionalities of that family, and altering them can change their semantics or corrupt the files. Embracing the analogy between these two distinct domains, we capitalize on the advanced alignment methods developed in bioinformatics. Our rationale is that – this alignment technique will capture code blocks that are common in one malware family the way it does for genomes in species.

The alignment technique identifies the common blocks, i.e., consensus sequences, per family, and estimates the degree of conservation at each location by processing the generated alignments. Then we generate a conservation score for each of these blocks depending on their conservation and frequency in that family. In this context, these aligned blocks along with their scores can be considered as the features for that corresponding malware family. However, there can be aligned common blocks that are shared in all malware families (for example, common PE header), and hence, they will not represent any family-specific functionalities. Therefore, we train a classifier on these generated conservation scores from these aligned blocks, including different families, so that the classifier learns the importance of these generated blocks for a specific family. During inference, to classify whether a new malware belongs to a family, we generate the alignment of this new malware with the previously generated common blocks of that family, and use it to compute a set of alignment scores. These scores are then fed to the classifier model to classify the new malware to its family.

Additionally, our adopted alignment approach can effectively handle addition, subtraction, substitution, and re-ordering in sequences, which provides *better robustness* to perturbation than conventional techniques. Furthermore, the use of such a back-trackable alignment approach with an *interpretable* ML model enables us to map its classification decision to the responsible suspicious code blocks. As a result, MALIGN is trustworthy for its decision which is highly crucial for malware applications.

Evaluation. We evaluate MALIGN for detecting malware families on two datasets: (i) Kaggle Microsoft Malware Classification Challenge (Big 2015) (Microsoft, 2015), and (ii) Microsoft Machine Learning Security Evasion Competition (2020) (MLSEC, 2020). In comparison to the state-of-the-art methods such as MalConv (Raff et al., 2018), CNN-based model (Kalash et al., 2018), and Feature-Fusion model (Ahmadi et al., 2016), our approach has higher accuracy, and the difference in performance is more noticeable when datasets are small. Using our auto-generated aligned blocks, i.e. consensus sequences, for each family, we backtracked to the exact code blocks that were responsible for our model decision. Thus, we were able to discover suspicious functionalities from malware samples, making our model explainable. Moreover, we theoretically prove that MALIGN is robust by-design to gradient attacks. We also evaluate the empirical robustness by generating adversarial malware using a gradient-based patch-append attack.

In summary, our main contributions are:

1. **Sequence alignment based approach.** We propose MALIGN by adopting sequence alignment concepts from bioinformatics into the static malware family classifier. We used a multiple sequence alignment-based tool to find conserved regions in raw binary executables (Section 4).
2. **High accuracy.** We evaluated MALIGN on two datasets, and it outperforms other state-of-the-art static detection methods. Besides, the performance gap gets higher with a lower amount of training data (Section 5).

²<https://dataprot.net/statistics/malware-statistics/>

³<https://www.comparitech.com/antivirus/malware-statistics-facts/>

3. **Explainable by-design.** Due to our design choice, MALIGN is backtrackable and explainable for its decision. We explore this in-depth and identify responsible code-blocks for multiple malware families. We share some of the interesting findings and insights that can help the security community (Section 6).
4. **Robust by-design.** We mathematically prove that our design choice makes MALIGN robust against gradient attacks. We also evaluate its empirical robustness against gradient-based patch attacks (Section 7).

2. Related Work

Machine Learning based classifiers. To counter the increasing amount of malware and detect them, several methods and techniques have been developed over the years. In the early days, Wressnegger et al. (2017) and Zakeri et al. (2015) proposed a signature-based approach using static analysis. Later, a dynamic approach - malware detection by analyzing the malware behavior, was proposed by Martignoni et al. (2008) and Willems et al. (2007). In recent times, machine learning based techniques are also being used to classify malware. Schultz et al. (2000) first proposed a data mining technique for malware detection using three different types of static features. Subsequently, Nataraj et al. (2011) proposed a malware classification approach based on image processing techniques by converting the bytes files to image files. Later, Kalash et al. (2018) improved on (Nataraj et al., 2011) by developing M-CNN using convolutional neural networks (CNN). Besides CNN, RNN has also been used for malware analysis. Shahzad et al. (2011) and Lu (2019) proposed techniques with LSTM using opcode sequences of malware. Santos et al. (2013) proposed a hybrid technique by integrating both static and dynamic analysis. Subsequently, Yan et al. (2018) developed MalNet using an ensemble of CNN, LSTM and by extracting metadata features, while Ahmadi et al. (2016) extracted and selected features of malware depending on the importance and applied feature fusion on them. Recently, Raff et al. (2018) developed a state-of-the-art technique MalConv using only the raw byte sequence as the input to a CNN-based deep-learning model.

Sequence Alignment based Classifiers. In the past, sequence alignment based approaches have been used for malware analysis by a number of researchers (Chen et al., 2012; Narayanan et al., 2012; Naidu and Narayanan, 2014; Kirat and Vigna, 2015; Naidu and Narayanan, 2016; Cho et al., 2016; Kim et al., 2019). Chen et al. (2012) used multiple sequence alignment to align computer viral and worm codes of variable lengths to identify invariant regions. This approach was subsequently enhanced later (Narayanan et al., 2012; Naidu and Narayanan, 2014, 2016). However, these approaches were not scalable enough to train on large malware sets and did not evaluate the robustness of their models, unlike our work.

Sequence alignment has also been applied on system call sequences of malware to extract evasion signatures and to cluster samples by Kirat and Vigna (2015), classification of malware families by Cho et al. (2016), and for malware detec-

tion, classification by D’Angelo et al. (2021), and visualization by Kim et al. (2019). Along with this line of work, there are existing works that proposed ensemble detection leveraging sequence alignment on API sequences (Ficco, 2021). All these approaches require access to API call sequences which require dynamic analysis and execution in a sandbox, virtual machine, or host. However, our proposed method is based on static analysis and only takes the raw bytes of a file which does not require any execution in a secondary machine.

Drew et al. (2016) utilized another approach developed by the bioinformatics and computational biology community and used gene or sequence classification methods for malware classification. The method is based on extracting short words i.e. k -mers from sequences and calculating the similarity between sequences based on the set of words present in them. Although the method is efficient, it does not fully utilize the information provided by stretches of conserved regions in malware and is not suitable for identifying critical code blocks in malware. In contrast, our method takes the whole raw-byte executable into consideration and so, can explain its decision by backtracking to the responsible code blocks.

Explainability of Models. Though there has been a large body of work on classifying and detecting malware, not much work has been done on explaining and interpreting the model decision. However, there are a few works that explored explainability, e.g., DREBIN (Arp et al., 2014), Melis et al. (2018, 2022), Backes and Nauman (2017), Kumar et al. (2018), Kinkead et al. (2021), MalDAE (Han et al., 2019), XMAL (Wu et al., 2021), etc. Unfortunately, all of these works were on Android malware using higher-level features like API calls, requested permissions, opcode sequences, etc., from manifest and disassembled code. In contrast, MALIGN takes raw-bytes from executables (Windows) and can explain the decision from that.

On the other hand, recent works in the machine learning community like LIME (Zhang et al., 2019), SHAP (Lundberg and Lee, 2017) propose strategies to interpret a decision of a blackbox model. However, these strategies assume that the local area of the classification boundary is linear. Later Guo et al. (2018a) proposed LEMNA showing that – when the decision boundary is non-linear, previous approaches would produce errors which makes them unsuitable for security applications. So, they solved this by using a mixture regression model enhanced by fused lasso. Though such models have played a great role in the explainability domain and inspired us, they have to be implemented and trained separately on a classifier model, which requires human engineering (like hyperparameter tuning) and adds computational overhead. However, our proposed method, MALIGN has a pipeline that is interpretable from top to bottom, i.e., easy to backtrack from decision output to problem space. Thus, it does not require any other model on top of it to explain its decision. Moreover, we generate signatures for each family that are easily interpretable by practitioners (see Section 6).

Adversarial Robustness. Continuous circumvention from malware authors and defense against such evasion by AV systems have turned into a never-ending cat-and-mouse game. For example, in the whitebox setting, Suciu et al. (2019), Kolos-

njaji et al. (2018), Kreuk et al. (2018b), Grosse et al. (2016), Al-Dujaili et al. (2018a), and in the blackbox setting, Demetrio et al. (2021), Ceschin et al. (2019), Fleshman et al. (2018b), Hu and Tan (2018), Rosenberg et al. (2018), Hu and Tan (2017), showed that adversarial attacks are effective against machine learning (ML) models in multiple ways. Also, Anderson et al. (2018), Song et al. (2020) proposed a reinforcement based approach to rewrite a binary for evading ML models.

Prior work proposed two main ways to improve the adversarial robustness of malware detectors: adversarial training and robustness by design. Adversarial training, where a malware detector is trained with adversarial examples, is one of the most commonly used approaches to improve adversarial robustness (Bai et al., 2021; Grosse et al., 2017; Zhang et al., 2021; Al-Dujaili et al., 2018b). However, such approaches hamper the classification accuracy, add computational overhead, and rely on the availability of enough adversarial samples, which may not always be the case in the fast-changing malware world (Lucas et al., 2023). So, in this work, we focus on the latter one – robustness by design.

Robustness by design approaches build classifiers to eliminate a certain class of adversarial attacks. For example, Chen et al. (2020) proposed learning PDF malware detectors with verifiable robustness properties, Saha et al. (2023) proposed a detector adopting the de-randomized smoothing scheme with certified robustness, Íncir Romeo et al. (2018) trained an XGBoost based malware detector with the monotonicity property, Fleshman et al. (2018a) trained a non-negative network to ensure that an adversary cannot decrease the classification score by adding extra content, etc. However, these approaches had to compromise the detection accuracy to some extent. For example, the non-negative MalConv model’s detection accuracy drops from 94.1% to 89.4%, while MALIGN can hold its performance as well as its robustness.

Moreover, recent works (Lucas et al., 2021, 2023) demonstrate the binary-diversification technique against new and old ML defenses. It is fundamental that – no ML model is fully robust against all attacks, and so it is better to not totally rely on ML models. So, we propose MALIGN that incorporates sequence alignment in front of ML models which makes it non-invertible and non-differentiable. We evaluate our model against a gradient-based attack and theoretically prove that it is robust-by-design.

3. Background

Sequence alignment is a widely studied problem in bioinformatics to find similarities among DNA, RNA, or protein sequences, and to study evolutionary relationships among diverse species. It is the process of arranging sequences in such a way that regions of similarity are *aligned*, with gaps (denoted by ‘-’) inserted to represent insertions and deletions in sequences. For example, an alignment of the sequences ATTGACCTGA and ATCGTGTA is shown below where the regions denoted in black, characterized by identical characters, are matched, whereas the red and blue regions denote substitutions i.e. point mutations,

and insertions or deletions during the evolutionary process, respectively.

```
ATTGACCTG-A
AT---CGTGTA
```

In sequence alignment, matches, mismatches, and insertions-deletions (in-dels) are assigned scores based on their frequencies during evolution and the goal is to find an alignment with the maximum score. The problem of finding an optimal alignment of the entire sequences (global alignment) and that of finding an optimal alignment of their sub-sequences (local alignment) can be solved by dynamic programming using the Needleman-Wunsch (Needleman and Wunsch, 1970) and the Smith-Waterman (Smith and Waterman, 1981) algorithms, respectively. While the algorithms can be used to align more than two sequences, the running time is exponential in the number of sequences. To address the tractability issue, a number of tools have been developed (Thompson et al., 1994; Katoh et al., 2002; Edgar, 2004), that use heuristics to solve the multiple sequence alignment (MSA) problem (wiki).

However, in addition to point mutations and short insertions-deletions, large scale genome rearrangement events take place during evolution. Such genome rearrangement events include reversal of a genomic segment (inversion), the shuffling of the order of genomic segments (transposition or translocation), duplication and deletion of segments, etc. Although the aforementioned tools are unable to deal with genome rearrangements, methods such as MUMmer (Delcher et al., 1999) can perform alignment of two sequences in the presence of rearrangements, whereas Mauve (Darling et al., 2004), Cactus (Paten et al., 2011), etc. can handle multiple sequences.

Recently, Armstrong et al. (2020) and Minkin and Medvedev (2020) have developed Progressive Cactus and SibeliaZ respectively, that can align hundreds to thousands of whole-genome sequences that may include rearrangements. The tools identify similar sub-sequences in the sequences from different species to create blocks of rearrangement-free sequences, and then perform a multiple sequence alignment of the sequences in each block.

Since adversaries can modify malware relatively easily by changing orders of blocks of codes without changing malware semantics, it is important that the tool used to align malware sequences is robust to such rearrangements in code. Here we use SibeliaZ to align malware sequences to identify conserved blocks of codes and calculate a conservation score of the blocks for malware family detection and classification (see Section 4). It is worth noting that the blocks of codes identified need not be fully conserved, i.e. there can be modifications, insertions, and deletions of a small number of instructions within the blocks, making it robust to adversarial attacks to some extent (see Section 7).

4. Methods

4.1. Overview

To classify known malware family and their variants, here we propose a malware family classification system based on

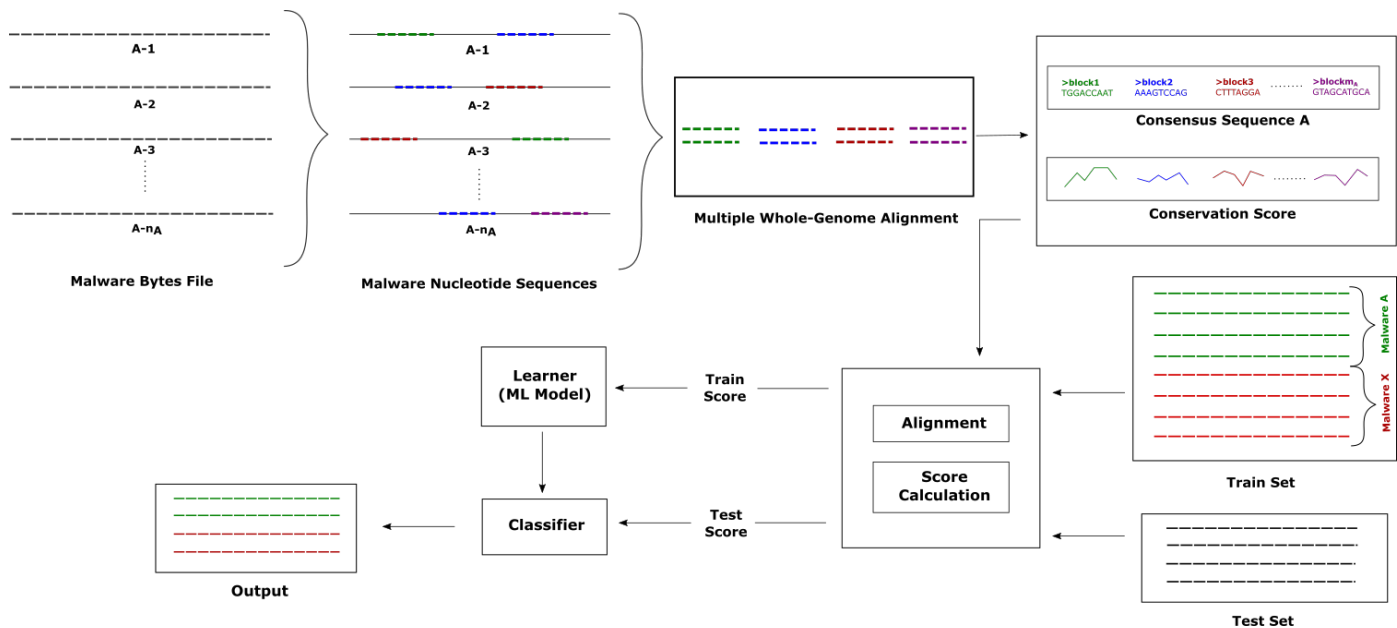


Figure 1: Overview of MALIGN. (1) The malware bytes files (executables) from malware of a particular family are first converted to nucleotide sequence files. (2) Then the malware nucleotide sequences are aligned using a multiple sequence alignment tool Sibeliaz. It first identifies similar sequences in different malware to form blocks. Highly similar sequences (colored sequences) can be in different orders in different files. The sequences in each block are then aligned. (3) The aligned sequences in each block are used to construct consensus sequences and conservation scores are calculated for each conserved block. (4) Then two sets of sequences - one corresponding to the malware family of interest and the other corresponding to non-malware or malware from other families are aligned to the consensus sequences and the degrees of conservation of each conserved block in the training sequences are estimated. (5) Finally a machine learning model is learnt to classify sequences based on the alignment scores of the sequences with the blocks. To classify new instances, sequences are aligned to the consensus sequences of the blocks and alignments are scored. The scores are then used as features for the class prediction.

multiple whole-genome alignment. The basic building block of the method is a binary classification system that can predict whether an executable belongs to a particular malware family or not. The input to this binary classifier is a training set consisting of positive samples i.e. malware from a particular family, and negative samples, which can be benign or malware from other families.

The main steps of our proposed method are shown in Algorithm 1 and an illustration is provided in Figure 1. We start with the given *malware bytes files*, i.e., PE files (Microsoft) and convert them to *malware nucleotide sequence files*, i.e., sequences of A, C, G, and T, to make them compatible with multiple whole-genome alignment technique (Sibeliaz (Minkin and Medvedev, 2020)). This outputs alignment blocks that are common among a number of these files. These alignment blocks are merged and thus *consensus sequence* is constructed. In this step, *conservation score* for each coordinate of the consensus sequence is also generated. This consensus sequence is aligned with each sample from a balanced training set with positive and negative samples with respect to the malware family of interest, and an *alignment score* is calculated for every sample for each conserved block. These scores are then used as input to a machine learning model, which learns a classifier to distinguish between malware belonging to the family and malware from other families. In the inference step, to classify a new sample, the sequence is aligned with the consensus sequence, and alignment scores for the new instance are generated in a similar way. The scores are passed into our classifier to classify

the new sample. Each of these steps is described in more detail below.

4.2. Bytes file to Nucleotide Sequence file Conversion

First, the binary executable or bytes files are converted to nucleotide sequence files containing sequences of A, C, G and T. The conversion is performed so that the existing whole-genome alignment tool can take the files as input. The conversion from the byte code to nucleotide sequence is done by converting each pair of bits to a nucleotide according to the following table:

| | |
|--------|--------|
| 00 → A | 01 → C |
| 10 → G | 11 → T |

Note that, similar conversions have been used by previous works, e.g. Naidu and Narayanan (2014, 2016); Drew et al. (2016), etc., and were successful in showing that such nucleotide sequences still can preserve necessary functionalities from the byte files.

In some malware datasets such as the Kaggle Microsoft Malware Classification Challenge (Big 2015) dataset (Microsoft, 2015), the provided bytes files contain “??” and long stretches of “00” in some cases which do not preserve any significant value or meaning. These are removed before the conversion to nucleotide sequences. Stretches of “00” longer than a threshold value of 32 were removed.

Algorithm 1: MALIGN

Input: Training set, $\mathbb{X} = (\mathbb{X}_+, \mathbb{X}_-)$, where \mathbb{X}_+ : byte files from malware of a family, \mathbb{X}_- : byte files from non-malware or malware from other families, and Test set, \mathbb{Y}

Output: Labels for \mathbb{Y}

$(\mathbb{S}_+, \mathbb{S}_-) \leftarrow$ Convert to nucleotide sequence files ($\mathbb{X}_+, \mathbb{X}_-$)

$\mathbb{B} \leftarrow$ Perform multiple sequence alignment and identify conserved blocks (\mathbb{S}_+)

forall blocks $B \in \mathbb{B}$ **do**

$C_B \leftarrow$ Get consensus sequence (B)

for $i = 1 \rightarrow \text{length}(B)$ **do**

 Calculate *ConservationScore*(B, i, N) where $N = A, C, G, T$

forall sequences $Z \in (\mathbb{S}_+ \cup \mathbb{S}_-)$ **do**

$F_Z :=$ Feature vector of Z

forall blocks $B \in \mathbb{B}$ **do**

$S \leftarrow$ Get alignments (Z, C_B)

$\text{AlignmentScore} \leftarrow$ Calculate alignment score (S, B)

$\text{AlignmentCount} \leftarrow$ Get alignment count (S)

$F_Z \leftarrow F_Z \cup (\text{AlignmentScore}, \text{AlignmentCount})$

$\mathcal{M} \leftarrow$ Learn classification model (\mathbb{F}, \mathbb{X}) where \mathbb{F} : feature matrix

$\mathbb{T} \leftarrow$ Convert to nucleotide sequence files (\mathbb{Y})

\mathbb{L} : labels

forall sequences $T \in \mathbb{T}$ **do**

$F_T :=$ Feature vector of T

forall blocks $B \in \mathbb{B}$ **do**

$S \leftarrow$ Get alignments (T, C_B)

$\text{AlignmentScore} \leftarrow$ Calculate alignment score (S, B)

$\text{AlignmentCount} \leftarrow$ Get alignment count (S)

$F_T \leftarrow F_T \cup (\text{AlignmentScore}, \text{AlignmentCount})$

$L \leftarrow$ Predict (\mathcal{M}, F_T)

$\mathbb{L} \leftarrow \mathbb{L} \cup L$

return \mathbb{L}

4.3. Multiple Alignment of Malware Nucleotide Sequences

The next step is to align the malware nucleotide sequences. In this paper, we adopt the multiple whole-genome alignment technique SibeliaZ (Minkin and Medvedev, 2020). It performs whole-genome alignment of multiple sequences and constructs locally co-linear blocks. Figure 2 illustrates alignment of three different malware nucleotide sequence files from the same family. The sequences share blocks of similar sequences shown in dashed lines of the same color. They may also contain sequences unique to each sequence indicated by lines with different colors.

During the block construction process: the order of the shared blocks may differ in different sequences and the blocks may not be fully shared across all sequences. This helps MALIGN to be robust against evasion attempts, such as reordering of instructions, injection of benign or random code at places, etc. In addition, the shared blocks may not be fully conserved, i.e., there can be mismatches of characters to some extent which means minor alteration or modification to the code will not prevent the detection of blocks. These properties of multiple whole-genome alignment improves the robustness of MALIGN against many evasion attacks.

SibeliaZ first identifies the shared linear blocks and then performs multiple sequence alignment of locally co-linear blocks. The block coordinates are output in the GFF format (wiki, 2023b) and the alignment is in the MAF format (Biopython). The multiple alignment format (MAF) is a format for describ-

ing multiple alignments in a way that is easy to parse and read. In our case, this format stores multiple alignment blocks at the byte code level among malware. We generate such an MAF file for each malware family using the training samples and identify the blocks of codes that are highly conserved across the malware family.

4.4. Consensus Sequence and Score Generation

We process all sequences of the alignment blocks of the MAF file from the previous step and generate a new sequence for each block, which we will call the *consensus sequence* – motivated by Kececioglu and Myers (1995). At first, we scan the length of all sequences and find the maximum one that will be the length of our consensus sequence. Then we traverse through the coordinates of every sequence and find the nucleotide of the highest occurrence for each coordinate. We put the most frequently occurring nucleotide at the corresponding index of the consensus sequence, i.e., the characters of the consensus sequences of the blocks are given by

$$C_{B,i} = \arg \max_{N \in \{A,C,G,T\}} k_{B,i,N}$$

for $1 \leq i \leq l_B$ and $B \in \mathbb{B}$, where $k_{B,i,N}$ is the count of the character $N (= A, C, G, T)$ at the i -th position in block B and l_B is the length of block B .

In Figure 2, consensus sequence generation of an alignment block (Block-1) is shown in detail. Below the alignment block, the corresponding sequence logo is shown. The height of the individual letters in the sequence logo represents how common the corresponding letter is at that particular coordinate of the alignment.

We thus construct the consensus sequence by taking the letter (nucleotide) with the highest frequency for each coordinate. Similarly, the consensus sequences for all blocks are generated and are stored in a file in FASTA (wiki, 2023a) format with a unique id. These consensus sequences are the conserved part of the malware family which can be considered as the signature or common pattern of that family. These files are later used to classify malware families.

In addition to the consensus sequence, we calculate *conservation scores* for the blocks. In bioinformatics, conservation score is used during the evaluation of sites in a multiple sequence alignment, in order to identify residues critical for structure or function. This is calculated per base, indicating how many species in a given multiple alignment match at each locus. We adopted this concept in the malware domain where the conservation score can indicate the significance or importance of a code segment in a malware family. The responsible code segments of malware will have high conservation scores compared to the segments that are not frequent or conserved in malware files.

In Figure 2, the heights of the bars corresponding to conservation scores indicate the degree of conservation at the corresponding positions. For each coordinate, we store the score for each of the four nucleotides which is given by the occurrence ratio of that nucleotide at that coordinate. So, *conservation*

sequences, the final score for first aligned sequence will be $21.96 (= 7.32 \times 3)$. Finally, the total alignment score for the block was calculated by adding the scores of all 3 aligned sequences.

In general, the *alignment score* of a sample Z for consensus sequence C_B of the block B is given by

$$\alpha_{Z,B} = \sum_{s \in S} \left(\sum_{i=1}^{\text{length}(s)} \gamma_{B,j,s_i} \right) \times n_B$$

where, S is the set of sequences from sample Z that got aligned to C_B , s_i is the i -th nucleotide of the sequence s , and j is the index of C_B where s_i was aligned.

Along with this score, we also store the total number of times the consensus sequence of a block gets aligned with the sample, i.e., *alignment count* $\beta_{Z,B} = |S|$. Both the number of occurrences and the total alignment score for the consensus sequence of each block for a malware family are used as input for the subsequent classification, resulting in $2m$ features if a malware family has m aligned blocks.

4.6. Classification

Finally, we train machine learning models for each malware family to classify malware. The scores and the number of alignments calculated as mentioned above are used as the features in our classifiers.

We experimented with a number of machine learning models including logistic regression, support vector machines (SVM), decision trees, and a simple deep learning model. Since the results did not vary significantly across models (see Table 2 in Results), we use logistic regression as our primary model for its better interpretability. We are going to refer this model as **MALIGN (Logistic Regression)** in the rest of this paper. We also experimented with a simple deep-learning model to find if it gives any better results, which we are going to refer to as **MALIGN (Deep Learning)**. However, such deep-learning models are not directly interpretable, and so, whenever we mention MALIGN in this paper, we indicate the MALIGN (Logistic Regression) version.

After the training phase, we get classifiers that can be used to classify new samples as shown in Figure 1. The scores of the training and the test samples are calculated in the same way. The scores for new samples are passed to the classifier for binary classification.

5. Evaluation

5.1. Datasets

5.1.1. The Kaggle Microsoft Malware Classification Challenge (Big 2015)

The Kaggle Microsoft Malware Classification Challenge (Big 2015) (Microsoft, 2015) aimed to organize a competition on malware family classification with a dataset consisting of 9 malware families (see Table 1).

This challenge simulates the data processed on over 160 million computers by Microsoft’s real-time anti-malware detection

products inspecting over 700 million computers per month. Microsoft provided almost half a terabyte of input training and classification input data when uncompressed. They included:

1. *Binary Files*: 10,868 training files containing the raw hexadecimal representation of the binary content of the malware.
2. *Assembly Files*: 10,868 training files containing data extracted by the Interactive Disassembler (IDA) tool. This information includes assembly command sequences, function calls, and more.
3. *Training Labels*: Each training file name is an MD5 hash of the actual program. Each MD5 hash and the malware class it maps to are stored in the training label file.

From this, we constructed 9 balanced datasets for binary classification consisting of an equal number of positive and negative samples for each of the 9 malware families. In each dataset, the positive examples are all the samples from the corresponding family and the negative examples were chosen by randomly sampling from the 8 other families in the dataset. Then 20% of each dataset was set aside as the test sets while the remaining 80% was used as the training sets. For the deep learning approaches that require hyper-parameter selection, the 80% was further split into training (60%) and validation sets (20%).

5.1.2. Microsoft Machine Learning Security Evasion Competition (2020) (MLSEC) Dataset

While the Kaggle Microsoft Malware Classification Challenge (Big 2015) dataset is a large and widely studied one, often new malware families only have a few samples - especially during their initial stages. Moreover, they might not always accurately represent real-world scenarios and in-the-wild practice. Therefore to assess the performance of our method on in-the-wild datasets with a small number of instances per family, we used the Microsoft Machine Learning Security Evasion Competition (2020) (MLSEC, 2020) dataset too.⁴

In this competition, the defenders’ challenge was to create a solution model that can defend against evasive variants created by the attackers. The defenders were provided a ‘Defender Challenge’ dataset with 49 original malware and their evasive variants created by real malware attackers. Each malware contains a different number of evasive variants varying from 5 to 20. On average, malware has 12 variants in this dataset. We chose this dataset because – i) it mirrors different types of real-life attacks, and ii) it has a limited number of samples which can be a good representation of new emerging malware.

Similarly to the Kaggle Microsoft Malware dataset, 49 different datasets were created for each family, which were then split into training, validation, and test sets. During the split of

⁴The dataset may not remain public by Microsoft by the time of publication, but we can provide the dataset upon request.

| Family Name | No of Train Samples | Type |
|----------------|---------------------|--------------------------------|
| Ramnit | 1541 | Worm |
| Lollipop | 2478 | Adware |
| Kelihos_ver3 | 2942 | Backdoor |
| Vundo | 475 | Trojan |
| Simda | 42 | Backdoor |
| Tracur | 751 | TrojanDownloader |
| Kelihos_ver1 | 398 | Backdoor |
| Obfuscator.ACY | 1228 | Any kind of obfuscated malware |
| Gatak | 1013 | Backdoor |

Table 1: Malware Families in the Kaggle Microsoft Malware Classification Challenge Dataset

this dataset, we always kept the original sample in the train set and the variants in the test set for each family, so that the test set can be considered as an evolution of the training set.

5.2. Evaluation of Machine Learning Algorithms

First, we assess the performance of various machine learning approaches on the Kaggle Microsoft Malware (Big 2015) dataset. The binary files of this dataset were converted to nucleotide sequence files and labeled using ‘Training Labels’ data provided by Microsoft. Then we generated common alignment blocks using SibeliaZ and constructed the consensus sequences as discussed in Section 4. We generated the conservation scores for each consensus sequences using the frequency of nucleotides which were then used as features for the machine learning models.

We experimented with logistic regression, decision trees, and support vector machines (SVM). Table 2 shows the test accuracy for 80%-20% train-test split on the Kaggle Microsoft Malware Classification Challenge (Big 2015) Dataset. We observe that the models show similar performances in terms of accuracy. So, we selected MALIGN (Logistic Regression) for future experiments because of its simplicity and interpretability. For hyper-parameters details and results on the train-set, readers can refer to Appendix A and Appendix B.

5.3. Comparison with Existing Approaches

Next, we compare the performance of MALIGN with some of the state-of-the-art approaches that can take raw-byte, MalConv (Raff et al., 2018) (a deep-learning based approach using raw byte sequence), Feature-Fusion (Ahmadi et al., 2016) (a feature extraction, selection and fusion based approach using byte and assembly files), and M-CNN (Kalash et al., 2018) (a CNN based approach relying on conversion to images) on the Kaggle Microsoft Malware (Big 2015) dataset. It is worth noting that models with multiclass loss as low as 0.00283 have been reported for this specific dataset. However, we compare with MalConv and M-CNN, as they have been successfully applied to many different datasets, and to our knowledge, the Feature-Fusion method has even better accuracy (multiclass logloss = 0.00128) than the winning team of the Kaggle competition. Besides simple ML models, we also implement a deep-learning based model on top of the alignment scores calculated

by MALIGN, which we refer to as MALIGN (Deep Learning). The architectures of the MALIGN (Deep Learning), MalConv and M-CNN are shown in Figure A.9 (see appendix).

The test and training accuracy of MALIGN with logistic regression and deep learning along with those of Feature-Fusion, MalConv, and M-CNN are shown in Tables 3 and B.11 (appendix). Table 3 shows that MALIGN (Deep Learning) has the best accuracy on the test set than other approaches. MALIGN (Logistic Regression) and (Deep Learning) have 97.99% and 98.59% accuracy which is close to the Kaggle winning team’s performance.

We compared MALIGN with other models with respect to recall, specificity, precision, and F1 score. Table 4 represents the overall performance of models taking the weighted average for all types (detailed result for each family in Table B.12 in the appendix). It shows that MALIGN has a more balanced performance than others. Moreover, it has higher precision which indicates that it has a comparatively low false positive rate – an indicator of a good malware detection model in commercial AV systems.

5.4. Applicability with Limited Amount of Data and Features

Although deep learning based approaches have been widely applied for malware classification and detection, they require extensive amounts of data for training and tend to overfit in the absence of that. Table 3 shows that Feature-Fusion, MalConv, and M-CNN perform arguably well for most malware families. However, we observe that, for Type 5 (Simda), which has only 42 samples, the test accuracies of Feature-Fusion, MalConv, and M-CNN are respectively 76.47%, 52.94% and 62.5% while MALIGN has 84.62% test accuracy. A similar observation can be made for Type 4 (Vundo) which has the second smallest number of training samples.

Moreover, MALIGN only needs the raw byte sequence whereas the typical methods like Feature-Fusion need other information or features, e.g., assembly file, address for byte sequence, section information from PE, etc. In addition, MALIGN can take any arbitrary length of input sequence whereas E2E deep learning based approach like MalConv, M-CNN suffers from limited input-length constraint.

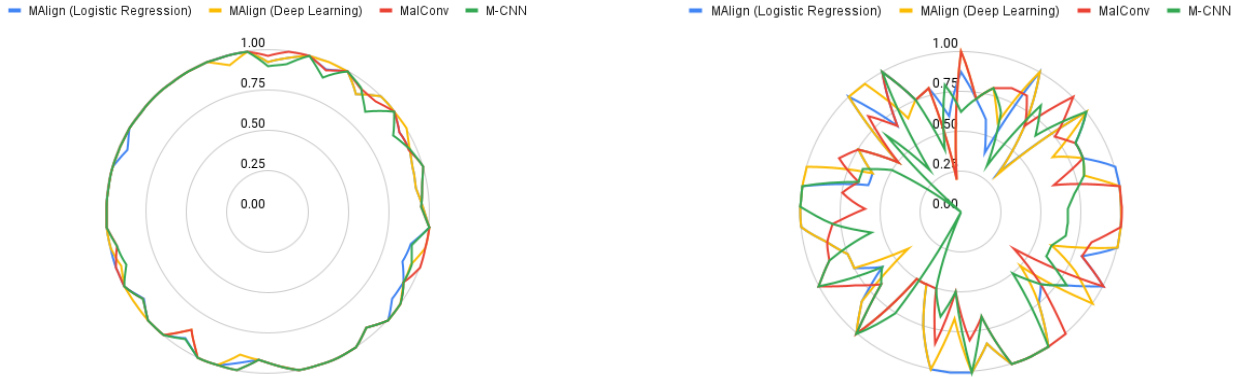
We also evaluated the performances of the methods on the MLSEC dataset (Microsoft Machine Learning Security Evasion

| Family Name | Test Accuracy | | |
|----------------|---------------------|---------------|-------|
| | Logistic regression | Decision tree | SVM |
| Ramnit | 99.64 | 99.82 | 99.64 |
| Kelihos_ver3 | 99.27 | 99.27 | 99.27 |
| Vundo | 97.4 | 97.4 | 97.4 |
| Simda | 84.62 | 84.62 | 84.62 |
| Tracur | 97.3 | 94.6 | 96.3 |
| Kelihos_ver1 | 96.7 | 98.9 | 98.9 |
| Obfuscator.ACY | 95.9 | 92.7 | 96 |
| Gatak | 96.2 | 96.2 | 96.2 |
| Overall | 97.99 | 97.42 | 98.02 |

Table 2: Test Accuracy on the Kaggle Dataset for different Machine Learning Models

| Family Name | MALIGN (Logistic Regression) | MALIGN (Deep Learning) | Feature-Fusion | MalConv | M-CNN |
|----------------|------------------------------|------------------------|----------------|---------|-------|
| Ramnit | 99.64 | 99.46 | 98.7 | 95.66 | 88.44 |
| Kelihos_ver3 | 99.27 | 99.82 | 99.18 | 100 | 99.72 |
| Vundo | 97.4 | 98.70 | 95.79 | 94.89 | 97.21 |
| Simda | 84.62 | 84.62 | 76.47 | 52.94 | 62.5 |
| Tracur | 97.3 | 98.2 | 98.34 | 93.91 | 94.55 |
| Kelihos_ver1 | 96.7 | 95.7 | 98.75 | 96.08 | 94.67 |
| Obfuscator.ACY | 95.9 | 96.39 | 98.98 | 94.42 | 91.74 |
| Gatak | 96.2 | 98.37 | 98.03 | 98.67 | 88.68 |
| Overall | 97.99 | 98.59 | 98.52 | 96.95 | 94.10 |

Table 3: Test Accuracy of all Models on the Kaggle Dataset



(a) Radar Chart showing Accuracy on MLSec-Train Dataset

(b) Radar Chart showing Accuracy on MLSec-Test Dataset

Figure 3: Radar Chart showing Accuracy of all Models along the perimeter on each of the individual 49 malware types in the MLSec Dataset

Competition (2020) (MLSEC, 2020)). Since it contains a limited number of variants created in almost real-time, this can be used to identify how our method works on new variants of a malware when only a limited number of samples are available. Because of the limited number of instances in this dataset, the validation set is very small for some types. Table 5 shows the weighted result of all models for an 80%-20% train-test split on all 49 malware families. Additionally, we evaluated another set of results for 60%-20%-20% train-validation-test split just for deep learning models (see Figure B.13 in appendix). We ob-

serve that MALIGN outperforms the other models on the MLSEC dataset regardless of the splitting.

Furthermore, Figures 3a and 3b provide radar charts that visually illustrate the training and test accuracy for all 49 types individually. From these figures, we observe that on the train set, all approaches have consistent performance, but on the test set M-CNN and MalConv are relatively inconsistent⁵. For example, types 29 and 43 have 10 and 5 available variants respectively, and M-CNN’s test accuracy is 0 on both, indicating a

| Model | Recall | Specificity | Precision | F1 Score |
|---------------------------------|--------------|--------------|--------------|--------------|
| MALIGN (Logistic Regression) | 96.66 | 98.60 | 98.67 | 97.61 |
| MALIGN (Deep Learning) | 99.00 | 98.18 | 98.19 | 98.59 |
| MalConv | 97.37 | 96.48 | 97.36 | 97.3 |
| M-CNN | 93.44 | 94.85 | 94.59 | 93.94 |

Table 4: Performance of Models on the Kaggle Dataset for other Evaluation Metrics

| Model | Train Accuracy | Test Accuracy |
|------------------------------|----------------|---------------|
| MALIGN (Logistic Regression) | 98.18 | 80.42 |
| MALIGN (Deep Learning) | 97.72 | 80.00 |
| Feature-Fusion | 98.02 | 60.94 |
| MalConv | 98.24 | 79.22 |
| M-CNN | 96.99 | 71.09 |

Table 5: Performance of Models on the MLSEC dataset for train-test split

limitation in its performance on these specific variants.

For further analysis, we experimented with dropping the train-set size of the Tracur family of the Kaggle dataset to half and evaluated all models. We observed that MALIGN has the least accuracy drop compared to others (see Table 6). Again, this proves the advantage of our method when a malware family does not have a considerably large sample size, which is very common in the case of emerging malware families. This was one of the motivations for adopting sequence alignment since its capability of explicit identification of critical code blocks still sustains the scarcity of data.

| Model | Accuracy Drop | Accuracy Change (%) ↓ |
|-----------------------------|-----------------|-----------------------|
| MALIGN(Logistic Regression) | 97.3% → 92.56% | 4.87% |
| MALIGN(Deep Learning) | 98.2% → 92.67% | 5.53% |
| MalConv | 93.91% → 85.67% | 8.77% |
| m-CNN | 94.55% → 83.22% | 11.98% |

Table 6: Test Accuracy Drop for dropping the train-set size of Tracur family to half

6. Explainability

An important feature of MALIGN which makes it different from other classifiers is its interpretability, and its capability of deriving suspicious code blocks in malware families through a simple *backtracking* process. Upon analysis, the ‘maliciousness’ of these suspicious code blocks can be determined. The *backtracking* process is as follows:

- (i) Finding the blocks that are assigned high weights by the logistic regression model.
- (ii) Selecting the blocks (found from step (i)) that are highly conserved.

⁵The more circular the perimeter line is, the more consistent the performance is.

- (iii) Processing the multiple alignment file (MAF) to find out the sequences and their indices that constructed the blocks.
- (iv) Locating the code fragments in binary and assembly files (using a disassembler) corresponding to the sequences found in step (iii).

We evaluated the interpretability of our MALIGN by following the above-mentioned backtracking process on multiple families from the Microsoft Kaggle Dataset ⁶. We discuss some of the interesting findings below (more in Appendix C).

6.1. Kelihos_ver1 Backdoor

The Kelihos backdoor allows the affected system to be part of the Kelihos botnet. It is then typically used to send spam email messages, steal information, etc. (fsecure, 2023a)

In our analysis of this specific backdoor malware, interestingly, one of our consensus sequences got mapped to 119 samples. While looking into the assembly code of this signature, we found that all of them are calling GetUserDefaultLangID function (see Figure 4). Usually, this function is called by malware to track geographical position and trigger a regional attack (malware function list).

Furthermore, we found more code blocks having suspicious Windows function calls from IEAdvpack.dll which gets abused by malware authors very often. From Figure C.13 in Appendix, we want to emphasize that – the order of these function calls is different in malwares, e.g., IsNTAdmin function is declared before RebootCheckOnInstall in C.13a and C.13b, but not in C.13c. However, MALIGN can successfully detect them due to its flexibility in alignment. The common pattern in these malwares from Figure C.13 is that – they are checking for admin privileges by IsNTAdmin, calling suspicious function RebootCheckOnInstall (also found in previous reports from Falcon Sandbox of CrowdStrike (2017, 2015)), and deleting files sometimes using DelNodeRunDLL32.

6.2. Tracur Trojan-Downloader

Trojan-Downloader:W32/Tracur.J is a malware that is known to identify a malicious DLL file that installs a plug-in for Internet Explorer and/or Mozilla Firefox web browsers and then redirects searches to an unsolicited website (fsecure, 2023c).

Consequently, malware authors write malware from Tracur family in such a way that it can get connected to the internet and download or upload the desired file (close to banking trojan (IOActive, 2012)). Our consensus sequence successfully detected code segments for such activities. Figure 5 is an example of such malware which is calling functions like – InternetReadFile, InternetCloseHandle. This clearly reveals that MALIGN is capable of capturing such sequential function calling that is suspicious.

⁶The MD5 hashes mentioned in this section are provided by the Kaggle Microsoft Dataset.

```

1  .text:00401B7F          ; ===== S U B R O U T I N E =====
2  .text:00401B7F          sub_401B7F      proc near          ; CODE XREF: sub_4015F8+3@CANp
3  .text:00401B7F          ; sub_401918+3@CANp ...
4  .text:00401B7F FF 35 14 20 40 00      push     ds:GetUserDefaultLangID
5  .text:00401B85 C3                    retn
6  .text:00401B85          sub_401B7F      endp                ; sp-analysis failed
7  .text:00401B85
8  .text:00401B86          ; -----
9  .text:00401B86 FF 35 18 20 40 00      push     ds:CreateMutexA
10 .text:00401B8C C3                    retn

```

Figure 4: Kelihos (version 1) Backdoor tracking user geological position for botnet connection(MD5 hash = aOCU2V7b0RkgQt9LfiYF)

```

1  .text:00402D4C FF 15 78 BE 45 00      call    InternetCloseHandle
2  .text:00402D52 33 C0                xor     eax, eax
3  .text:00402D54 E9 07 01 00 00        jmp     loc_402E60
4  .text:00402D59          ; -----
5  .text:00402D59
6  .text:00402D59          loc_402D59:          ; CODE XREF: sub_402CDF+5F@CANj
7  .text:00402D59          ; sub_402CDF+68@CANj ...
8  .text:00402D59 68 FF 0F 00 00        push    0FFFh        ; size_t
9  .text:00402D5E 8D 85 E5 EF FF FF      lea    eax, [ebp+var_101B]
10 .text:00402D64 53                    push    ebx           ; int
11 .text:00402D65 50                    push    eax           ; void *
12 .text:00402D66 89 5D FC              mov    [ebp+var_4], ebx
13 .text:00402D69 88 9D E4 EF FF FF      mov    [ebp+var_101C], bl
14 .text:00402D6F E8 2C 13 00 00        call   memset
15 .text:00402D74 83 C4 0C              add    esp, 0Ch
16 .text:00402D77 8D 45 FC              lea    eax, [ebp+var_4]
17 .text:00402D7A 50                    push    eax
18 .text:00402D7B 68 00 10 00 00        push    1000h
19 .text:00402D80 8D 85 E4 EF FF FF      lea    eax, [ebp+var_101C]
20 .text:00402D86 50                    push    eax
21 .text:00402D87 FF 75 F8              push    [ebp+var_8]
22 .text:00402D8A FF 15 70 BE 45 00      call    InternetReadFile
23 .text:00402D90 3B C3                cmp    eax, ebx
24 .text:00402D92 0F 84 87 00 00 00      jz     loc_402E1F
25 .text:00402D98 39 5D FC              cmp    [ebp+var_4], ebx
26 .text:00402D9B 76 6C                jbe    short loc_402E09
27 .text:00402D9D 3B F3                cmp    esi, ebx
28 .text:00402D9F 75 1C                jnz    short loc_402DBD
29 .text:00402DA1 53                    push    ebx

```

Figure 5: Tracur Trojan-Downloader trying to read file from internet (MD5 hash = gEZCMz90lrmlI8cx37FNT)

6.3. Obfuscator.ACY

Malware with vastly different purposes often “obfuscate” i.e. hide its purpose so that security software does not detect it (Microsoft, 2017). While different obfuscator tools can obfuscate or protect the malicious code in different ways, some packers like *Themida* keep one function – `TlsSetValue` (Borges, 2020) so that it can unpack it later. This function is used to set the value of a pointer allocated for a TLS variable and has been heavily used by malware authors for many different attacks (Hellal and Romdhane, 2016; Poudyal and Dasgupta, 2021), e.g., stack-smashing attack (Nebenzahl et al., 2006).

In our analysis, we found consensus sequences getting matched with code blocks that contain `TlsSetValue`. Figure 6 shows the code block from one of such consensus sequences which was present in 39 samples from *Obfuscator.ACY* family.

6.4. Vundo Trojan

Vundo is malware that downloads and displays pop-up advertisements of rogue software. It can download and install other malware and there are variants that collect information such as IP address, MAC address, Windows and browser versions, etc. and send it to attackers (FireEye, 2008-2014).

While analyzing random malware executables from *Vundo* family, surprisingly, we found some consensus sequences that were mapped to binary sequences from different sections. To evaluate whether they are just some spurious features or not, we examined their assembly code and interestingly found that there is obfuscated code (from `DllEntryPoint` function) put into the ‘data’ section instead of ‘text’ section. It might be the case that – one malware is loading another in its data section. However, such patterns got identified by our MALIGN since their binary representations are similar (see Figures C.11 and C.10 in Appendix).

6.5. Simda Backdoor

Backdoor:W32/Simda is a large malware family that allows attackers to remotely control machines they are installed in to steal personal or system data, take screenshots, download additional files onto the system, etc. (fsecure, 2023b)

Among the MALIGN generated consensus sequences for *Simda* family, we randomly selected some of them and found matches to some suspicious function calls. For example, two samples had exactly the same code where they were declaring suspicious functions like – `LookupPrivilegeValueW`, `CreateProcessAsUserW`, `SetTokenInformation`, etc.

```

1  .data:004155E6 4C 6F 61 64 4C 69 62 72+      db 'LoadLibraryA',0
2  .data:004155F3 00                          align 4
3  .data:004155F4 4E 03                        word_4155F4      dw 34Eh          ; DATA XREF: .data:00415480@CANo
4  .data:004155F6 54 6C 73 53 65 74 56 61+      db 'TlsSetValue',0
5  .data:00415602 7E 03                        word_415602      dw 37Eh          ; DATA XREF: .data:0041547C@CANo

```

Figure 6: Detection of non-removable TlsSetValue function by Obfuscator tool (MD5 hash = IjoyeRsfBXW3bOUDMARL)

```

1  .rdata:0040BB8C 47 65 74 54 6F 6B 65 6E 49 6E+      db 'GetTokenInformation',0
2  .rdata:0040BBA0 2D 00                        word_40BBA0      dw 2Dh          ; DATA XREF: .rdata:0040B484@CANo
3  .rdata:0040BBA2 43 6F 6E 76 65 72 74 53 74 72+      db 'ConvertStringSecurityDescriptorToSecurityDescriptorW',0
4  .rdata:0040BBD7 00                          align 4
5  .rdata:0040BBD8 20 01                        word_40BBD8      dw 120h         ; DATA XREF: .rdata:0040B488@CANo
6  .rdata:0040BBD9 4C 6F 6F 6B 75 70 50 72 69 76+      db 'LookupPrivilegeValueW',0
7  .rdata:0040BBF0 04 01                        word_40BBF0      dw 104h         ; DATA XREF: .rdata:0040B48C@CANo
8  .rdata:0040BBF2 43 72 65 61 74 65 50 72 6F 63+      db 'CreateProcessAsUserW',0
9  .
10 .
11 .rdata:0040BC5C 47 65 74 55 73 65 72 4E 61 6D+      db 'GetUserNameW',0
12 .rdata:0040BC69 00                          align 2
13 .rdata:0040BC6A 20 01                        word_40BC6A      dw 120h         ; DATA XREF: .rdata:0040B4A4@CANo
14 .rdata:0040BC6C 53 65 74 54 6F 6B 65 6E 49 6E+      db 'SetTokenInformation',0
15 .rdata:0040BC80 41 44 56 41 50 49 33 32 2E 44+      aAdvapi32_dll db 'ADVAPI32.DLL',0 ; DATA XREF: .rdata:0040B260@CANo

```

Figure 7: Suspicious function calls that matched with our consensus sequence for Simda Backdoor(MD5 hash = hrguW0CqMt2mJdfvX8IB)

Then, they are using ADVAPI32.DLL through which they can access core windows components such as the service manager and registry (see Figure 7). It might be the case that the backdoor malware is checking for the privilege to perform privileged operations, or checking if the privilege escalation exploit should be executed later.

7. Robustness

A major issue with static malware detection approaches is - they can be evaded by malware authors in multiple ways, such as adding content without altering malware functionalities. There are several ways to find or generate this content, such as gradient-based patch (Kreuk et al., 2018b; Kolosnjaji et al., 2018; Suciú et al., 2019). Since MALIGN relies on finding conserved blocks critical to the malware families for classification through sequence alignment and score calculation, and an interpretable logistic regression model, it should in principle to be inherently robust to such attacks.

7.1. Theoretical Robustness

To formally show the difficulty of such attacks, as in Pierazzi et al. (2020); Guo et al. (2018b), we mathematically prove that inverting our whole genome alignment process is an NP-Hard problem.

7.1.1. Proof

| Symbol | Description |
|-----------|---|
| Z | Problem space (i.e., input space) |
| X | Feature Space |
| Y | Label Space |
| φ | Feature mapping function, $\varphi : Z \rightarrow X$ |
| g | Classifier, $g : X \rightarrow Y$ |

Table 7: Symbols with Description

We consider problem space Z that contains malware files z each having a ground truth label $y \in Y$. The feature mapping function φ , i.e., the alignment tool, score generation algorithm, etc, maps the input z to a feature vector x ; $\varphi(z) = x$. The machine learning classifier predicts a label y for x ; $g(x) = y$.

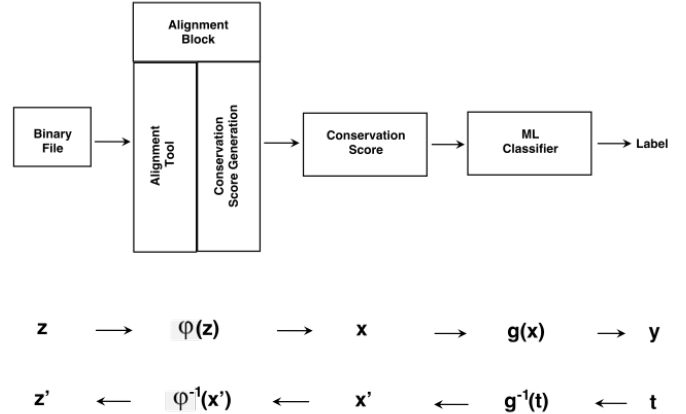


Figure 8: Flow of our method and the backward flow for attacks

Let's consider that all training and classifying algorithm is disclosed to the attacker. The attacker's goal would be to perturb the input z to z' in such a way that our model misclassifies it as label t , where $t \neq y$. Since the machine learning classifier is a differentiable model, it is possible to find perturbed feature vector x' through the gradient attack, such that, $g^{-1}(t) = x'$. The next job of the attacker would be to find an inverse feature mapping function, such that $\varphi^{-1}(x') = z'$. Now to block this backward flow, the feature mapping function φ needs to be non-invertible and non-differentiable.

Hardness of Invertibility

Let, $B = \{B_1, B_2, B_3, \dots, B_m\}$ denote the set of m alignment blocks of a malware family where each element B_i is a string

of nucleotides. The i^{th} alignment block B_i is represented by a conservation score matrix $A_i \in [0, 1]^{5 \times n}$ which stores the conservation scores for each nucleotide, where n is the length of the block. So, each row of the score matrix A will store the scores for A, C, G, T and gap, respectively.

Let, $S_i = \{S_i^1, S_i^2, S_i^3, \dots, S_i^c\}$ denote the set of sequences from perturbed malware file z' that got aligned with alignment block B_i for c times. Let's assume, without loss of generality, that only one sequence from input z' is aligned with alignment block B_i and so only one alignment score α_{z, B_i} is generated.

So, to prove the hardness of invertibility, it suffices to prove that reconstructing the alignment sequence S_i from the conservation score matrix A_i and the alignment score α_{z, B_i} is hard i.e. the following problem is NP-hard.

Alignment Inversion Problem: Given a conservation score matrix $A \in [0, 1]^{5 \times n}$ and a target alignment score α , the alignment inversion problem is to find $y_{i,j} \in \{0, 1\}^{5 \times n}$ such that

$$\sum_{i=1}^5 \sum_{j=1}^n y_{i,j} A_{i,j} = \alpha$$

Here the conservation scores for each column in matrix A is normalized, i.e., $\sum_{i=1}^5 A_{i,j} = 1$ for all j .

In order to show that the Alignment Inversion Problem is NP-hard, we reduce a well-known NP-complete problem, the subset sum problem, to our problem.

Subset Sum Problem: The subset sum problem (SSP) is, given a set of integers and a target sum T , to decide whether any subset of the integers sum to T . The problem is NP-complete even when the numbers are restricted to positive integers. So, SSP refers to finding variables $(x_1, x_2, x_3, \dots, x_n) \in \{0, 1\}^n$, given positive integers $(a_1, a_2, a_3, \dots, a_n) \in \mathbb{N}^n$ and T , such that

$$\sum_{j=1}^n x_j a_j = T$$

Now, given an SSP instance, we generate an instance of the alignment inversion problem by setting

$$A_{1,j} = \frac{a_j}{N}, A_{5,j} = 1 - \frac{a_j}{N}, A_{i,j} = 0 \text{ for } i = \{2, 3, 4\}$$

$$\text{and } \alpha = \frac{T}{N}$$

Here N is a positive integer chosen to make sure that i) $0 \leq A_{i,j} \leq 1$ for all i, j , and ii) $A_{5,j} = 1 - \frac{a_j}{N} \geq \alpha$ for all j . This can be done by setting

$$N > a_{\max} + T$$

where $a_{\max} = \max(a_1, a_2, \dots, a_n)$.

Since $A_{5,j} \geq \alpha$ for all j , none of the scores for gaps can be included in the target alignment score α , and $A_{i,j}$ for $i = 2, 3, 4$ cannot contribute towards α as they are set to 0. Therefore, given the solution to the instance of one problem, we can obtain the solution to the other by setting $x_j = A_{1,j}$ for all j , because of the following:

$$\sum_{j=1}^n x_j a_j = T \iff \frac{1}{N} \sum_{j=1}^n x_j a_j = \frac{T}{N} \iff \sum_{j=1}^n y_{1,j} A_{1,j} = \alpha$$

Since SSP is a NP-hard problem and polynomial-time reducible to our problem, our problem is a NP-hard problem too. In our original problem, we may have to consider multiple nucleotides in most cases which is a harder version of this instance. So, it is trivial to prove that, our original problem is a NP-hard problem too.

While we acknowledge that – theoretical robustness does not ensure practical robustness, this property of MALIGN shows that the model is robust to certain kinds of attack.

7.2. Empirical Robustness

We also investigated the empirical robustness of our method compared to the other conventional malware detection techniques. We generated adversarial malwares using gradient-based patch attack of Kolosnjaji et al. (2018). It creates adversarial samples just by modifying (or padding) approximately 1.25% of the total size of malware which can successfully evade⁷ the MalConv model with a high percentage. The evasion rate increases with the percentage of modification on malware samples. We experimented with their implementation ([github link](#)) on some of the types in the MLSEC dataset.

| Type | MalConv | | MALIGN | |
|------|------------------------|-----------------------|--------------|--------------|
| | Evaded/Total Train set | Evaded/Total Test set | Evasion Rate | Evasion Rate |
| 1 | 5/15 | 2/4 | 36.84% | 0.00% |
| 11 | 1/9 | 1/2 | 18.18% | 0.00% |
| 12 | 5/13 | 2/4 | 41.18% | 0.00% |
| 28 | 5/8 | 2/2 | 70% | 0.00% |
| 45 | 4/5 | 2/2 | 85.71% | 0.00% |

Table 8: Evasion Rate on MalConv and MALIGN using Gradient-based patch attack for some types in the MLSEC Dataset

We then applied these evasive samples on MALIGN and all of them were successfully detected with almost 100% prediction confidence (see Table 8). The probable reason for such a difference in the evasion rate is – gradient-based patch attack (Kolosnjaji et al., 2018) appends random bytes at the end of a malware file to evade the classifier, and since the alignment mechanism of MALIGN is robust to insertions, its decision remains unaltered. Moreover, due to the non-invertible property of MALIGN (proved in subsection 7.1.1), the attacker cannot generate any such random content with gradient approach to evade it.

It is worth mentioning that – no static analyzer can provide robustness to all type of attacks (similarly, no attack can evade all defense models). So, as security researchers, our goal is to make the bar higher for attackers. Since MALIGN finds conserved code blocks in the presence of substitutions, insertions, and deletions of instructions, modifying those code segments sufficiently while preserving the malware semantics will be more challenging than other used models. However, we have discussed more about evasion techniques for MALIGN in the [Appendix D.1](#).

⁷If a malware gets detected by a model but its adversarial version gets undetected, then we call it a ‘successful evasion’.

8. Running Time

For our experiments, we used a CPU of 40GB memory and GeForce RTX 3090. MALIGN only requires the CPU, whereas we had to use the GPU for the deep learning based methods.

8.1. Mean-Time-To-Detect (MTTD)

| Method | MTTD | Training Time |
|---------|-------------|---------------|
| MALIGN | 0.0112584 s | 18hr 4min |
| MalConv | 1.2461524 s | 18hr 13min |
| M-CNN | 0.8706633 s | 14hr 26min |

Table 9: MTTD and training time for different methods on the MLSEC dataset

We evaluated the MTTD for all methods by considering the time they take in their inference stage. We ran all methods on the test set of the MLSEC dataset and measured the total time for the classifier to make the decisions. Then we divided this time by the total number of samples in the test set to find the MTTD.

Table 9 shows the MTTD for each method. Since MalConv and M-CNN are deep learning models unlike MALIGN (Logistic Regression), they take comparatively more time to classify a sample. Notably, we did not include the feature extraction time here, for which MALIGN takes 15.9498 seconds on average. In this feature extraction step, the graph construction step by TwoPaCo (Minkin et al., 2017) takes up to 12 seconds which is 75.24% of the whole process. Since we do not have any control over the implementation of TwoPaCo, we cannot speed this process up anymore. However, once the signatures are found in MALIGN, they can be trimmed if needed (based on how conserved they are) and then the alignment of the sequence of the new instance and the signature will be faster.

8.2. Training Time

We also evaluated the total training time for each method on the MLSEC dataset. From Table 9, we can see that the training time is not vastly different from other methods. Here, we have included the time for alignment and feature extraction too.

Ahmadi et al. (2016)’s Feature-Fusion method has not been included in Table 9 because for the MLSEC dataset, partial features (only features from byte code) were considered. But we can get an estimation of its running time on the Kaggle Microsoft dataset from the original paper (Ahmadi et al., 2016). For example, it takes almost 17 hours and 15 minutes to extract only the ‘REG’ feature from all samples, and it has to extract 14 features in total.

9. Discussion

In this work, we proposed MALIGN for malware family classification from raw executables – distinct from the prior works in this domain for its interpretability and better robustness. To show that MALIGN can actually help the AV security practitioners in real-life, we analyzed a vast number of potentially suspicious code blocks found from our consensus sequences, and

upon analysis, we evaluated their maliciousness depending on the context. Some of them have been shared in Section 6 and Appendix C (after getting double-checked by a security analyst from a reputed AV company). Besides, we also generated some statistics on our consensus sequence analysis (see Appendix E).

9.1. Limitations

The approach used in MALIGN has some limitations too. Firstly, though with recent and efficient multiple sequence alignment tools like SibeliaZ (Minkin and Medvedev, 2020) we can align malware files very fast, the time can grow with the number of samples in a family. Secondly, any static analyzer is fundamentally vulnerable since it cannot execute and analyze the behavior of the malware. Though MALIGN provides robustness against some specific attacks, such as gradient-based patch attacks, it might not be the case for all attacks (discussed in Appendix D.1). Thirdly, like most other static analyzers, it cannot perform on packed and encrypted malware without unpacking or decrypting it.

10. Conclusion

In this paper, we presented a malware family classification tool MALIGN adopting a recently developed multiple whole-genome alignment tool SibeliaZ. Sequence alignment based approaches have been used for malware analysis in the past, but the use of a whole-genome alignment tool makes MALIGN scalable to long malware sequences and protects against trivial adversarial attacks. The method is also interpretable and can be used to derive insights on malware such as the identification of critical code blocks and code obfuscation. To our knowledge, we are the first to explore the interpretability on a raw-byte based static malware classifier.

We have applied MALIGN on the Kaggle Microsoft Malware Classification Challenge (Big 2015) and the Microsoft Machine Learning Security Evasion Competition (2020) (MLSec) datasets, and observed that it outperforms state-of-the-art static classifier methods such as the MalConv, Feature-Fusion, and M-CNN method. However, outperforming other models is not the main goal of this paper, rather we wanted to explore static analysis from a different perspective to balance accuracy, interpretability, and robustness.

We discovered malicious code-blocks from our consensus sequences that can provide insights to malware analysts. We welcome security practitioners to utilize MALIGN for not only classifying but also analyzing the malware. MALIGN can be used in the future to measure the variance among malware samples which might provide insights about common practices by malware authors. We believe it might open up a new paradigm in the malware analysis domain.

Code Availability

Our code can be found here - <https://github.com/ShoumikSaha/Malign>

CRedit authorship contribution statement

- **Shoumik Saha:** Conceptualization, Data curation, Formal Analysis, Methodology, Software, Validation, Visualization, Writing – original draft, Writing – review & editing
- **Sadia Afroz:** Resources, Supervision, Writing – review & editing
- **Atif Hasan Rahman:** Conceptualization, Formal Analysis, Investigation, Resources, Supervision, Writing – review & editing

Acknowledgements

We would like to express our sincere gratitude to Erin Avl-lazagaj for his review and feedback. He helped us to improve the paper by analyzing some signatures.

References

- Ahmadi, M., Ulyanov, D., Semenov, S., Trofimov, M., Giacinto, G., 2016. Novel feature extraction, selection and fusion for effective malware family classification, in: Proceedings of the sixth ACM conference on data and application security and privacy, pp. 183–194.
- Al-Dujaili, A., Huang, A., Hemberg, E., O’Reilly, U.M., 2018a. Adversarial deep learning for robust detection of binary encoded malware, in: 2018 IEEE Security and Privacy Workshops (SPW), IEEE. pp. 76–82.
- Al-Dujaili, A., Huang, A., Hemberg, E., O’Reilly, U.M., 2018b. Adversarial deep learning for robust detection of binary encoded malware, in: 2018 IEEE Security and Privacy Workshops (SPW), IEEE. pp. 76–82.
- Anderson, B., Quist, D., Neil, J., Storlie, C., Lane, T., 2011. Graph-based malware detection using dynamic analysis. *Journal in computer Virology* 7, 247–258.
- Anderson, H.S., Kharkar, A., Filar, B., Evans, D., Roth, P., 2018. Learning to evade static pe machine learning malware models via reinforcement learning. *arXiv preprint arXiv:1801.08917*.
- Armstrong, J., Hickey, G., Diekhans, M., Fiddes, I.T., Novak, A.M., Deran, A., Fang, Q., Xie, D., Feng, S., Stiller, J., et al., 2020. Progressive Cactus is a multiple-genome aligner for the thousand-genome era. *Nature* 587, 246–251.
- Arp, D., Spreitzenbarth, M., Hubner, M., Gascon, H., Rieck, K., Siemens, C., 2014. Drebin: Effective and explainable detection of android malware in your pocket., in: *Ndss*, pp. 23–26.
- AV-Test, 2023. Av-test malware statistics. URL: <https://www.av-test.org/en/statistics/malware/>.
- Avllazagaj, E., Zhu, Z., Bilge, L., Balzarotti, D., Dumitras, T., 2021. When malware changed its mind: An empirical study of variable program behaviors in the real world, in: 30th USENIX Security Symposium (USENIX Security 21), pp. 3487–3504.
- Backes, M., Nauman, M., 2017. Luna: quantifying and leveraging uncertainty in android malware analysis through bayesian machine learning, in: 2017 IEEE European symposium on security and privacy (euos&p), IEEE. pp. 204–217.
- Bai, T., Luo, J., Zhao, J., Wen, B., Wang, Q., 2021. Recent advances in adversarial training for adversarial robustness. *arXiv preprint arXiv:2102.01356*.
- Biopython, . Multiple alignment format. https://biopython.org/wiki/Multiple_Alignment_Format.
- Borges, A., 2020. Handling advanced threats. URL: <http://tinyurl.com/bdhdz5xd>.
- Ceschin, F., Botacin, M., Gomes, H.M., Oliveira, L.S., Grégio, A., 2019. Shallow security: On the creation of adversarial variants to evade machine learning-based malware detectors, in: Proceedings of the 3rd Reversing and Offensive-oriented Trends Symposium, pp. 1–9.
- Chen, Y., Narayanan, A., Pang, S., Tao, B., 2012. Multiple sequence alignment and artificial neural networks for malicious software detection, in: 2012 8th International Conference on Natural Computation, IEEE. pp. 261–265.
- Chen, Y., Wang, S., She, D., Jana, S., 2020. On training robust {PDF} malware classifiers, in: 29th {USENIX} Security Symposium ({USENIX} Security 20), pp. 2343–2360.
- Cho, I.K., Kim, T.G., Shim, Y.J., Ryu, M., Im, E.G., 2016. Malware analysis and classification using sequence alignments. *Intelligent Automation & Soft Computing* 22, 371–377.
- CrowdStrike, 2015. Falcon sandbox report on 927.exe. URL: <https://tinyurl.com/2s97ccjr>.
- CrowdStrike, 2017. Falcon sandbox report on freepdf4.12.exe. URL: <https://tinyurl.com/5xmx2tzk>.
- CrowdStrike, 2018-2019. Falcon sandbox report on bakcdoor. <https://tinyurl.com/3h8px5b9>, <https://tinyurl.com/ymnt6rsy>.
- Darling, A.C., Mau, B., Blattner, F.R., Perna, N.T., 2004. Mauve: multiple alignment of conserved genomic sequence with rearrangements. *Genome Research* 14, 1394–1403.
- Delcher, A.L., Kasif, S., Fleischmann, R.D., Peterson, J., White, O., Salzberg, S.L., 1999. Alignment of whole genomes. *Nucleic Acids Research* 27, 2369–2376.
- Demetrio, L., Biggio, B., Lagorio, G., Roli, F., Armando, A., 2021. Functionality-preserving black-box optimization of adversarial windows malware. *IEEE Transactions on Information Forensics and Security* 16, 3469–3478.
- Drew, J., Moore, T., Hahsler, M., 2016. Polymorphic malware detection using sequence classification methods, in: 2016 IEEE Security and Privacy Workshops (SPW), IEEE. pp. 81–87.
- D’Angelo, G., Ficco, M., Palmieri, F., 2021. Association rule-based malware classification using common subsequences of api calls. *Applied Soft Computing* 105, 107234. URL: <https://www.sciencedirect.com/science/article/pii/S1568494621001575>, doi:<https://doi.org/10.1016/j.asoc.2021.107234>.
- Edgar, R.C., 2004. MUSCLE: multiple sequence alignment with high accuracy and high throughput. *Nucleic Acids Research* 32, 1792–1797.
- Ficco, M., 2021. Malware analysis by combining multiple detectors and observation windows. *IEEE Transactions on Computers* 71, 1276–1290.
- FireEye, 2008-2014. Fireeye vundo trojan. URL: <https://mil.fireeye.com/edp.php?sname=Trojan.Vundo>.
- Fleshman, W., Raff, E., Sylvester, J., Forsyth, S., McLean, M., 2018a. Non-negative networks against adversarial attacks. *arXiv preprint arXiv:1806.06108*.
- Fleshman, W., Raff, E., Zak, R., McLean, M., Nicholas, C., 2018b. Static malware detection & subterfuge: Quantifying the robustness of machine learning and current anti-virus, in: 2018 13th International Conference on Malicious and Unwanted Software (MALWARE), IEEE. pp. 1–10.
- fsecure, 2023a. Backdoor.kelihos by f-secure. URL: https://www.f-secure.com/v-descs/backdoor_w32_kelihos.shtml.
- fsecure, 2023b. Backdoor:w32/simda by f-secure. URL: https://www.f-secure.com/v-descs/backdoor_w32_simda.shtml.
- fsecure, 2023c. Trojan-downloader:w32/tracur.j by f-secure. URL: https://www.f-secure.com/v-descs/trojan-downloader_w32_tracur_j.shtml.
- Grosse, K., Papernot, N., Manoharan, P., Backes, M., McDaniel, P., 2016. Adversarial perturbations against deep neural networks for malware classification. *arXiv preprint arXiv:1606.04435*.
- Grosse, K., Papernot, N., Manoharan, P., Backes, M., McDaniel, P., 2017. Adversarial examples for malware detection, in: European symposium on research in computer security, Springer. pp. 62–79.
- Guo, W., Mu, D., Xu, J., Su, P., Wang, G., Xing, X., 2018a. Lemna: Explaining deep learning based security applications, in: proceedings of the 2018 ACM SIGSAC conference on computer and communications security, pp. 364–379.
- Guo, W., Wang, Q., Zhang, K., Ororbia, A.G., Huang, S., Liu, X., Giles, C.L., Lin, L., Xing, X., 2018b. Defending against adversarial samples without security through obscurity, in: 2018 IEEE International Conference on Data Mining (ICDM), IEEE. pp. 137–146.
- Han, W., Xue, J., Wang, Y., Huang, L., Kong, Z., Mao, L., 2019. Maldae: Detecting and explaining malware based on correlation and fusion of static and dynamic characteristics. *computers & security* 83, 208–233.

- Hellal, A., Romdhane, L.B., 2016. Minimal contrast frequent pattern mining for malware detection. *Computers & Security* 62, 19–32.
- Hu, W., Tan, Y., 2017. Generating adversarial malware examples for black-box attacks based on gan. *arXiv preprint arXiv:1702.05983*.
- Hu, W., Tan, Y., 2018. Black-box attacks against rnn based malware detection algorithms, in: *Workshops at the Thirty-Second AAAI Conference on Artificial Intelligence*.
- Huang, A., Al-Dujaili, A., Hemberg, E., O'Reilly, U.M., 2018. On visual hallmarks of robustness to adversarial malware. *arXiv preprint arXiv:1805.03553*.
- Íncar Romeo, Í., Theodorides, M., Afroz, S., Wagner, D., 2018. Adversarially robust malware detection using monotonic classification, in: *Proceedings of the Fourth ACM International Workshop on Security and Privacy Analytics*, pp. 54–63.
- IOActive, 2012. Reversal and analysis of zeus and spyeye banking trojans.
- JoeSandbox, 2023. Joesandbox report on bakdoor. URL: <https://www.joesandbox.com/analysis/821041/0/html#>.
- Kalash, M., Rochan, M., Mohammed, N., Bruce, N.D., Wang, Y., Iqbal, F., 2018. Malware classification with deep convolutional neural networks, in: *2018 9th IFIP International Conference on New Technologies, Mobility and Security (NTMS)*, IEEE. pp. 1–5.
- Kato, K., Misawa, K., Kuma, K.I., Miyata, T., 2002. MAFFT: a novel method for rapid multiple sequence alignment based on fast Fourier transform. *Nucleic Acids Research* 30, 3059–3066.
- Kececioğlu, J.D., Myers, E.W., 1995. Combinatorial algorithms for dna sequence assembly. *Algorithmica* 13, 7–51.
- Kim, H., Kim, J., Kim, Y., Kim, I., Kim, K.J., Kim, H., 2019. Improvement of malware detection and classification using api call sequence alignment and visualization. *Cluster Computing* 22, 921–929.
- Kinthead, M., Millar, S., McLaughlin, N., O’Kane, P., 2021. Towards explainable cnns for android malware detection. *Procedia Computer Science* 184, 959–965.
- Kirat, D., Vigna, G., 2015. Malgene: Automatic extraction of malware analysis evasion signature, in: *Proceedings of the 22nd ACM SIGSAC Conference on Computer and Communications Security*, pp. 769–780.
- Kolosnjaji, B., Demontis, A., Biggio, B., Maiorca, D., Giacinto, G., Eckert, C., Roli, F., 2018. Adversarial malware binaries: Evading deep learning for malware detection in executables, in: *2018 26th European signal processing conference (EUSIPCO)*, IEEE. pp. 533–537.
- Kreuk, F., Barak, A., Aviv-Reuven, S., Baruch, M., Pinkas, B., Keshet, J., 2018a. Deceiving end-to-end deep learning malware detectors using adversarial examples. *arXiv preprint arXiv:1802.04528*.
- Kreuk, F., Barak, A., Aviv-Reuven, S., Baruch, M., Pinkas, B., Keshet, J., 2018b. Deceiving end-to-end deep learning malware detectors using adversarial examples. *arXiv preprint arXiv:1802.04528*.
- Kumar, R., Xiaosong, Z., Khan, R.U., Kumar, J., Ahad, I., 2018. Effective and explainable detection of android malware based on machine learning algorithms, in: *Proceedings of the 2018 International Conference on Computing and Artificial Intelligence*, pp. 35–40.
- github link, <https://github.com/yuxiaorun/MalConv-Adversarial>.
- malware function list, *Windows functions in malware analysis*. URL: <https://gist.github.com/404NetworkError/a81591849f5b6b5fe09f517efc189c1d#isntadmin-top>.
- Liu, Y., Tantithamthavorn, C., Li, L., Liu, Y., 2022. Explainable ai for android malware detection: Towards understanding why the models perform so well?, in: *2022 IEEE 33rd International Symposium on Software Reliability Engineering (ISSRE)*, IEEE. pp. 169–180.
- Lu, R., 2019. Malware detection with lstm using opcode language. *arXiv preprint arXiv:1906.04593*.
- Lucas, K., Pai, S., Lin, W., Bauer, L., Reiter, M.K., Sharif, M., 2023. Adversarial training for raw-binary malware classifiers.
- Lucas, K., Sharif, M., Bauer, L., Reiter, M.K., Shintre, S., 2021. Malware makeover: Breaking ml-based static analysis by modifying executable bytes, in: *Proceedings of the 2021 ACM Asia Conference on Computer and Communications Security*, pp. 744–758.
- Lundberg, S.M., Lee, S.I., 2017. A unified approach to interpreting model predictions. *Advances in neural information processing systems* 30.
- Marcus, G., 2018. Deep learning: A critical appraisal. *arXiv preprint arXiv:1801.00631*.
- Martignoni, L., Stinson, E., Fredrikson, M., Jha, S., Mitchell, J.C., 2008. A layered architecture for detecting malicious behaviors, in: *International Workshop on Recent Advances in Intrusion Detection*, Springer. pp. 78–97.
- Melis, M., Maiorca, D., Biggio, B., Giacinto, G., Roli, F., 2018. Explaining black-box android malware detection, in: *2018 26th european signal processing conference (EUSIPCO)*, IEEE. pp. 524–528.
- Melis, M., Scalas, M., Demontis, A., Maiorca, D., Biggio, B., Giacinto, G., Roli, F., 2022. Do gradient-based explanations tell anything about adversarial robustness to android malware? *International journal of machine learning and cybernetics*, 1–16.
- Microsoft, . Microsoft PE format. URL: <https://learn.microsoft.com/en-us/windows/win32/debug/pe-format>.
- Microsoft, 2015. Microsoft malware classification challenge (big 2015). <https://www.kaggle.com/c/malwareclassification/>.
- Microsoft, 2017. *Virtool:win32/obfuscator.acy* by microsoft. URL: <https://www.microsoft.com/en-us/wdsi/threats/malware-encyclopedia-description?Name=VirTool:Win32/Obfuscator.ACY>.
- Minkin, I., Medvedev, P., 2020. Scalable multiple whole-genome alignment and locally collinear block construction with SibeliaZ. *Nature communications* 11, 1–11.
- Minkin, I., Pham, S., Medvedev, P., 2017. Twopaco: an efficient algorithm to build the compacted de bruijn graph from many complete genomes. *Bioinformatics* 33, 4024–4032.
- MLSEC, 2020. Microsoft machine learning security evasion competition. <https://www.microsoft.com/en-us/security/blog/2021/07/29/attack-ai-systems-in-machine-learning-evasion-competition/>.
- Naidu, V., Narayanan, A., 2014. Further experiments in biocomputational structural analysis of malware, in: *2014 10th International Conference on Natural Computation (ICNC)*, IEEE. pp. 605–610.
- Naidu, V., Narayanan, A., 2016. Needleman-wunsch and smith-waterman algorithms for identifying viral polymorphic malware variants, in: *2016 IEEE 14th Intl Conf on Dependable, Autonomic and Secure Computing, 14th Intl Conf on Pervasive Intelligence and Computing, 2nd Intl Conf on Big Data Intelligence and Computing and Cyber Science and Technology Congress (DASC/PiCom/DataCom/CyberSciTech)*, IEEE. pp. 326–333.
- Narayanan, A., Chen, Y., Pang, S., Tao, B., 2012. The effects of different representations on malware motif identification, in: *2012 Eighth International Conference on Computational Intelligence and Security*, IEEE. pp. 86–90.
- Nataraj, L., Karthikeyan, S., Jacob, G., Manjunath, B.S., 2011. Malware images: visualization and automatic classification, in: *Proceedings of the 8th international symposium on visualization for cyber security*, pp. 1–7.
- Nebenzahl, D., Sagiv, M., Wool, A., 2006. Install-time vaccination of windows executables to defend against stack smashing attacks. *IEEE Transactions on Dependable and Secure Computing* 3, 78–90.
- Needleman, S.B., Wunsch, C.D., 1970. A general method applicable to the search for similarities in the amino acid sequence of two proteins. *Journal of Molecular Biology* 48, 443–453.
- Or-Meir, O., Nissim, N., Elovici, Y., Rokach, L., 2019. Dynamic malware analysis in the modern era—a state of the art survey. *ACM Computing Surveys (CSUR)* 52, 1–48.
- Pascanu, R., Stokes, J.W., Sanossian, H., Marinescu, M., Thomas, A., 2015. Malware classification with recurrent networks, in: *2015 IEEE International Conference on Acoustics, Speech and Signal Processing (ICASSP)*, IEEE. pp. 1916–1920.
- Paten, B., Earl, D., Nguyen, N., Diekhans, M., Zerbino, D., Haussler, D., 2011. Cactus: Algorithms for genome multiple sequence alignment. *Genome Research* 21, 1512–1528.
- Petti, S., Bhattacharya, N., Rao, R., Dauparas, J., Thomas, N., Zhou, J., Rush, A.M., Koo, P.K., Ovchinnikov, S., 2021. End-to-end learning of multiple sequence alignments with differentiable smith-waterman. *BioRxiv*.
- Pierazzi, F., Pendlebury, F., Cortellazzi, J., Cavallaro, L., 2020. Intriguing properties of adversarial ml attacks in the problem space, in: *2020 IEEE Symposium on Security and Privacy (SP)*, pp. 1332–1349. doi:10.1109/SP40000.2020.00073.
- Poudyal, S., Dasgupta, D., 2021. Analysis of crypto-ransomware using ml-based multi-level profiling. *IEEE Access* 9, 122532–122547.
- Raff, E., Barker, J., Sylvester, J., Brandon, R., Catanzaro, B., Nicholas, C.K., 2018. Malware detection by eating a whole exe, in: *Workshops at the Thirty-Second AAAI Conference on Artificial Intelligence*, pp. 268–276.
- Rosenberg, I., Shabtai, A., Rokach, L., Elovici, Y., 2018. Generic black-box end-to-end attack against state of the art api call based malware classifiers,

in: International Symposium on Research in Attacks, Intrusions, and Defenses, Springer. pp. 490–510.

Saha, S., Wang, W., Kaya, Y., Feizi, S., Dumitras, T., 2023. Drsm: Derandomized smoothing on malware classifier providing certified robustness. [arXiv:2303.13372](https://arxiv.org/abs/2303.13372).

Santos, I., Devesa, J., Brezo, F., Nieves, J., Bringas, P.G., 2013. Opem: A static-dynamic approach for machine-learning-based malware detection, in: International joint conference CISIS'12-ICEUTE' 12-SOCO' 12 special sessions, Springer. pp. 271–280.

Schultz, M.G., Eskin, E., Zadok, F., Stolfo, S.J., 2000. Data mining methods for detection of new malicious executables, in: Proceedings 2001 IEEE Symposium on Security and Privacy. S&P 2001, IEEE. pp. 38–49.

Shahzad, R.K., Lavesson, N., Johnson, H., 2011. Accurate adware detection using opcode sequence extraction, in: 2011 Sixth International Conference on Availability, Reliability and Security, IEEE. pp. 189–195.

Smith, T.F., Waterman, M.S., 1981. Identification of common molecular subsequences. *Journal of Molecular Biology* 147, 195–197.

Song, W., Li, X., Afroz, S., Garg, D., Kuznetsov, D., Yin, H., 2020. Malmalware: A reinforcement learning framework for attacking static malware classifiers. *arXiv preprint arXiv:2003.03100*.

Suciu, O., Coull, S.E., Johns, J., 2019. Exploring adversarial examples in malware detection, in: 2019 IEEE Security and Privacy Workshops (SPW), IEEE. pp. 8–14.

Thompson, J.D., Higgins, D.G., Gibson, T.J., 1994. CLUSTAL W: improving the sensitivity of progressive multiple sequence alignment through sequence weighting, position-specific gap penalties and weight matrix choice. *Nucleic Acids Research* 22, 4673–4680.

wiki, . Multiple sequence alignment. https://en.wikipedia.org/wiki/Multiple_sequence_alignment.

wiki, 2023a. Fasta format. https://en.wikipedia.org/wiki/FASTA_format.

wiki, 2023b. General Feature format. URL: https://en.wikipedia.org/wiki/General_feature_format.

Willems, C., Holz, T., Freiling, F., 2007. Toward automated dynamic malware analysis using cwsandbox. *IEEE Security & Privacy* 5, 32–39.

Wressnegger, C., Freeman, K., Yamaguchi, F., Rieck, K., 2017. Automatically inferring malware signatures for anti-virus assisted attacks, in: Proceedings of the 2017 ACM on Asia Conference on Computer and Communications Security, pp. 587–598.

Wu, B., Chen, S., Gao, C., Fan, L., Liu, Y., Wen, W., Lyu, M.R., 2021. Why an android app is classified as malware: Toward malware classification interpretation. *ACM Transactions on Software Engineering and Methodology (TOSEM)* 30, 1–29.

Yan, J., Qi, Y., Rao, Q., 2018. Detecting malware with an ensemble method based on deep neural network. *Security and Communication Networks* 2018.

Zakeri, M., Faraji Daneshgar, F., Abbaspour, M., 2015. A static heuristic approach to detecting malware targets. *Security and Communication Networks* 8, 3015–3027.

Zhang, Y., Li, H., Zheng, Y., Yao, S., Jiang, J., 2021. Enhanced dnns for malware classification with gan-based adversarial training. *Journal of Computer Virology and Hacking Techniques* 17, 153–163.

Zhang, Y., Song, K., Sun, Y., Tan, S., Udell, M., 2019. " why should you trust my explanation?" understanding uncertainty in lime explanations. *arXiv preprint arXiv:1904.12991*.

Appendix A. Models

Appendix A.1. Hyperparameters for Machine Learning Models

We experimented with the hyper-parameters for our machine learning models. The finding for each model are given below –

Appendix A.1.1. Logistic Regression

We got the best results for ‘elasticnet’ penalty, $C=0.05$ (regularization factor), ‘saga’ solver and $l1_ratio=0.5$.

Appendix A.1.2. Decision Tree

We got the best result with ‘gini’ criterion, ‘best’ splitter, ‘none’ max_depth keeping the min_samples_split=5.

Appendix A.1.3. Support Vector Machine (SVM)

We found that the SVM classifier performed best for $C=0.005$ (regularization factor) and ‘linear’ kernel.

Appendix A.2. Hyperparameters for Deep Learning Models

Appendix A.2.1. MalConv Model

For the MalConv model, we followed the similar implementation of the original paper (Raff et al., 2018). We used SGD with Nesterov momentum with 0.01 learning rate and 0.9 momentum. We set the max input length to 2MB and 8 samples per batch. We trained the model for 20 epochs.

Appendix A.2.2. M-CNN model

For the M-CNN model, we used the same backbone and hyperparameters mentioned in the original paper (Kalash et al., 2018). We used VGG-16 as the backbone setting the learning rate to 0.001 with 0.9 momentum. We trained the model for 20 epochs.

Appendix A.2.3. Feature-Fusion Model

For this model, we used the implementation that was made available on github by Ahmadi et al. (2016) in their paper. We used ‘random forest’ as the classifier.

Appendix A.3. Deep Learning Model Architectures

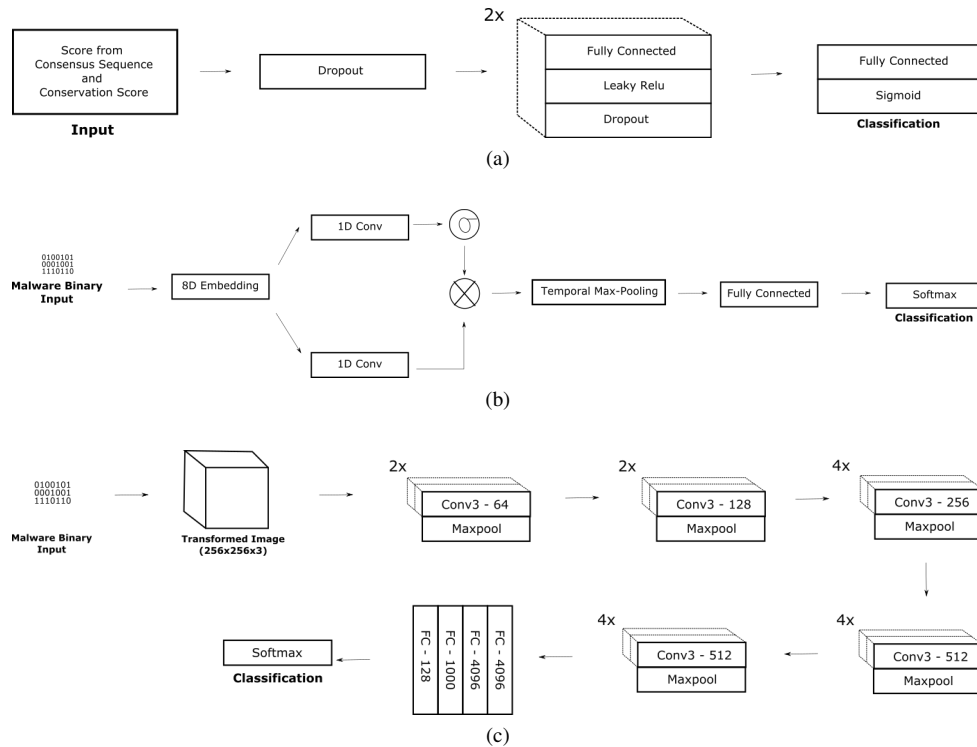


Figure A.9: Architectures of (a) MALIGN (Deep Learning) model, (b) MalConv model Raff et al. (2018), and (c) M-CNN model Kalash et al. (2018).

Appendix B. Result Tables

| Family Name | Train Accuracy | | |
|----------------|---------------------|---------------|-------|
| | Logistic regression | Decision tree | SVM |
| Ramnit | 99.91 | 99.91 | 99.91 |
| Kelihos_ver3 | 99.83 | 99.94 | 99.81 |
| Vundo | 100 | 100 | 100 |
| Simda | 100 | 100 | 97.92 |
| Tracur | 100 | 100 | 99.5 |
| Kelihos_ver1 | 100 | 100 | 99.5 |
| Obfuscator.ACY | 100 | 100 | 100 |
| Gatak | 99.17 | 99.17 | 99.17 |
| Overall | 99.82 | 99.86 | 99.74 |

Table B.10: Training Accuracy on Kaggle Microsoft Malware Dataset for Different Machine Learning Models

| Family Name | MALIGN (Logistic Regression) | MALIGN (Deep Learning) | Feature-Fusion | MalConv | M-CNN |
|----------------|---------------------------------|---------------------------|----------------|---------|-------|
| Ramnit | 99.91 | 99.58 | 100 | 98.39 | 97.64 |
| Kelihos_ver3 | 99.83 | 99.86 | 100 | 99.89 | 99.91 |
| Vundo | 100 | 98.26 | 100 | 99.4 | 99.26 |
| Simda | 100 | 94.44 | 100 | 100 | 100 |
| Tracur | 100 | 98.18 | 100 | 98.74 | 98.43 |
| Kelihos_ver1 | 100 | 98.92 | 100 | 98.54 | 99.52 |
| Obfuscator.ACY | 100 | 98.66 | 100 | 97.33 | 99.70 |
| Gatak | 99.17 | 99.2 | 100 | 99.15 | 92.69 |
| Overall | 99.82 | 99.24 | 100 | 98.96 | 98.4 |

Table B.11: Training Accuracy of different models on Kaggle Microsoft Malware Classification Challenge Dataset

| Family Name | MALIGN (Logistic Regression) | | | MalConv | | | M-CNN | | |
|----------------|---------------------------------|--------------|--------------|--------------|-------------|------------|--------------|--------------|--------------|
| | Recall | Specificity | Precision | Recall | Specificity | Precision | Recall | Specificity | Precision |
| Ramnit | 99.65 | 99.63 | 99.65 | 96.75 | 94.81 | 94.9 | 90.26 | 86.36 | 86.88 |
| Kelihos_ver3 | 98.98 | 99.32 | 99.32 | 100 | 100 | 100 | 100 | 99.32 | 99.32 |
| Vundo | 91.67 | 100 | 100 | 96.15 | 93.06 | 95.24 | 98.55 | 96.36 | 94.44 |
| Simda | 100 | 71.43 | 75 | 52.94 | 0 | 100 | 54.54 | 80 | 85.71 |
| Tracur | 89.29 | 100 | 100 | 91.62 | 98 | 98.79 | 94.49 | 94.57 | 91.96 |
| Kelihos_ver1 | 98.04 | 95.24 | 96.15 | 96.29 | 95.83 | 96.29 | 90.79 | 98.65 | 98.57 |
| Obfuscator.ACY | 94.53 | 97.52 | 97.58 | 97.5 | 91.15 | 92.12 | 89.03 | 94.47 | 94.19 |
| Gatak | 95.05 | 97.03 | 96.97 | 97.61 | 100 | 100 | 84.08 | 93.85 | 93.89 |
| Overall | 96.66 | 98.60 | 98.67 | 97.37 | 96.48 | 97.36 | 93.44 | 94.85 | 94.59 |

Table B.12: Performance of different models on Test-set of Kaggle Microsoft Malware Classification Challenge Dataset for other evaluation metrics

| Models | Train Accuracy | Validation Accuracy | Test Accuracy |
|------------------------|----------------|---------------------|---------------|
| MALIGN (Deep Learning) | 97.53 | 81.67 | 79.58 |
| Feature-Fusion | 96.83 | 58.59 | 62.50 |
| MalConv | 95.39 | 81.22 | 64.45 |
| M-CNN | 98.4 | 74.29 | 73.83 |

Table B.13: Performance of Deep Learning Models on MLSEC Dataset for train-validation-test split

Appendix C. Explainability

Appendix C.1. Vundo Trojan

We found multiple consensus sequences, i.e. signatures of MALIGN, for Vundo Trojan family where code obfuscation was being used by malware authors. Here, we show two such examples in Figures C.10 and C.11. In both of them, we found the same binary sequence being used in `.text` and `.data` section of PE files. We suspect that – one malware sample is loading another by keeping the code in its `.data` section.

```

1  .text:10002562          loc_10002562:          ; CODE XREF: DllEntryPoint:loc_10002534(CAN)
2  .text:10002562 03 F2          add     esi, edx
3  .text:10002564 EB 17          jmp     short loc_1000257D
4  .text:10002566          ; -----
5  .text:10002566 9C          pushf
6  .text:10002567 A5          movsd
7  .text:10002568          ; -----
8  .text:10002568          loc_10002568:          ; CODE XREF: DllEntryPoint:loc_1000257D(EM)
9  .text:10002568 EB 2B          jmp     short loc_10002595
10 .text:10002568          ; -----
11 .text:1000256A 7A 2B          dw     2B7Ah
12 .text:1000256C 88 21 46 07 34 5D D2 A3 A0 59 1E FF CC 15 2A 1B          dd     7462188h, 0A3D25D34h, 0FF1E59A0h, 1B2A15CC
13 .text:1000257C B8          db     0B8h
14 .text:1000257D          ; -----
15 .text:1000257D          ; -----
16 .text:1000257D          loc_1000257D:          ; CODE XREF: DllEntryPoint+1564(CAN)
17 .text:1000257D EB E9          jmp     short loc_10002568
18 .text:1000257D          ; -----
19 .text:1000257F 91          db     91h
20 .text:10002580 F6 F7 64 CD          dd     0CD64F7F6h

```

(a) Code in `.text` segment (MD5 hash = jEZkrOP7GayNmiXdget5)

```

1  .data:10005E95 3C          db     3Ch ; <
2  .data:10005E96 24          db     24h ; $
3  .data:10005E97 EB          db     0EBh ; ë
4  .data:10005E98 17          db     17h
5  .data:10005E99 9C          db     9Ch ; œ
6  .data:10005E9A A5          db     0A5h ; ¥
7  .data:10005E9B EB          db     0EBh ; ë
8  .data:10005E9C 2B          db     2Bh ; +
9  .data:10005E9D 7A          db     7Ah ; z
10 .data:10005E9E 2B          db     2Bh ; +
11 .data:10005E9F 88          db     88h ; ^
12 .data:10005EA0 21          db     21h ; !
13 .data:10005EA1 46          db     46h ; F
14 .data:10005EA2 07          db     7
15 .data:10005EA3 34          db     34h ; 4
16 .data:10005EA4 5D          db     5Dh ; j
17 .data:10005EA5 D2          db     0D2h ; Ò
18 .data:10005EA6 A3          db     0A3h ; ã
19 .data:10005EA7 A0          db     0A0h ;
20 .data:10005EA8 59          db     59h ; Y
21 .data:10005EA9 1E          db     1Eh
22 .data:10005EAA FF          db     0FFh
23 .data:10005EAB CC          db     0CCh ; Ĭ
24 .data:10005EAC 15          db     15h
25 .data:10005EAD 2A          db     2Ah ; *
26 .data:10005EAE 1B          db     1Bh
27 .data:10005EAF B8          db     0B8h ; ,
28 .data:10005EB0 EB          db     0EBh ; ë
29 .data:10005EB1 E9          db     0E9h ; é
30 .data:10005EB2 91          db     91h ; `
31 .data:10005EB3 F6          db     0F6h ; ö
32 .data:10005EB4 F7          db     0F7h ; ÷
33 .data:10005EB5 64          db     64h ; d

```

(b) Code in `.text` segment (MD5 hash = kRUx3TuoJGp0sqDzNGX)

Figure C.10: Code obfuscation in Vundo Trojan. (a) and (b) have the same code in `.text` and `.data` section, respectively

```

1  .text:1000457A CB                retf
2  .text:1000457B                ; -----
3  .text:1000457B A8 C1            test    al, 0C1h
4  .text:1000457D                ; -----
5  .text:1000457D                loc_1000457D:                ; CODE XREF: DllEntryPoint:loc_1000458B[EM]
6  .text:1000457D EB 2F            jmp     short loc_100045AE
7  .text:1000457D                ; -----
8  .text:1000457F 66                db     66h
9  .text:10004580 A7 54 FD F2 43 C0 F9 3E dd     0F2FD54A7h, 3EF9C043h
10 .text:10004588 9F EC B5            db     9Fh, 0ECh, 0B5h
11 .text:1000458B                ; -----
12 .text:1000458B                loc_1000458B:                ; CODE XREF: DllEntryPoint:loc_10004560[CAN]
13 .text:1000458B                jmp     short loc_1000457D
14 .text:1000458B EB F0            ; -----
15 .text:1000458B                ; -----
16 .text:1000458D 4A BB D8            db     4Ah, 0BBh, 0D8h
17 .text:10004590                ; -----
18 .text:10004590 31 16            xor     [esi], edx
19 .text:10004592                ; -----
20 .text:10004592                loc_10004592:                ; CODE XREF: DllEntryPoint:loc_100045AE[EM]
21 .text:10004592 EB 2D            jmp     short loc_100045C1
22 .text:10004592                ; -----
23 .text:10004594 97 84 6D A2 33 F0 69 EE 8F dd     0A26D8497h, 0EE69F033h, 0FA251C8Fh
24 .text:10004594 1C 25 FA AB 08 A1 C6+ dd     0C6A108ABh, 52DDB487h
25 .text:10004594 87 B4 DD 52 23 20 D9 9E dd     9ED92023h
26 .text:100045AC 7F 4C            db     7Fh, 4Ch

```

(a) Code in .text segment (MD5 hash = g7vEfrR3s49CH8AVUeSu)

```

1  .text:10007370 CB                retf
2  .text:10007371                ; -----
3  .text:10007371 A8 C1            test    al, 0C1h
4  .text:10007373 66 A7            cmpsw
5  .text:10007375 54                push   esp
6  .text:10007376 FD                std
7  .text:10007377                ; -----
8  .text:10007377                loc_10007377:                ; CODE XREF: sub_10006B8C:loc_10007381[EM]
9  .text:10007377 EB 2B            jmp     short loc_100073A4
10 .text:10007377                ; -----
11 .text:10007379 F2 43 C0            db     0F2h, 43h, 0C0h
12 .text:1000737C F9 3E 9F EC            dd     0EC9F3EF9h
13 .text:10007380 B5                db     0B5h
14 .text:10007381                ; -----
15 .text:10007381                loc_10007381:                ; CODE XREF: sub_10006B8C:loc_10007342[CAN]
16 .text:10007381                jmp     short loc_10007377
17 .text:10007381 EB F4            ; -----
18 .text:10007383                ; -----
19 .text:10007383 4A                dec     edx
20 .text:10007384 BB D8 31 16 97 mov     ebx, 971631D8h
21 .text:10007389 84 6D A2            test   [ebp-5Eh], ch
22 .text:1000738C                ; -----
23 .text:1000738C                loc_1000738C:                ; CODE XREF: sub_10006B8C:loc_100073A4[EM]
24 .text:1000738C EB 29            jmp     short loc_100073B7
25 .text:1000738C                ; -----
26 .text:1000738E 33 F0            dw     0F033h
27 .text:10007390 69 EE 8F 1C 25 FA AB 08 dd     1C8FEE69h, 8ABFA25h,
28 .text:10007390 A1 C6 87 B4 DD 52 23 20+ dd     0B487C6A1h, 202352DDh, 4C7F9ED9h

```

(b) Code in .text segment (MD5 hash = Gpd5s3Y7HKwXf4NaOPZk)

| | | | | | |
|----|-------------------|--------------|----|-------------------|--------------|
| 1 | .data:1000792A CB | db 0CBh ; È | 26 | .data:10007943 2D | db 2Dh ; - |
| 2 | .data:1000792B A8 | db 0A8h ; " | 27 | .data:10007944 97 | db 97h ; - |
| 3 | .data:1000792C C1 | db 0C1h ; Å | 28 | .data:10007945 84 | db 84h ; „ |
| 4 | .data:1000792D EB | db 0EBh ; ë | 29 | .data:10007946 6D | db 6Dh ; m |
| 5 | .data:1000792E 2F | db 2Fh ; / | 30 | .data:10007947 A2 | db 0A2h ; ¢ |
| 6 | .data:1000792F 66 | db 66h ; f | 31 | .data:10007948 33 | db 33h ; 3 |
| 7 | .data:10007930 A7 | db 0A7h ; \$ | 32 | .data:10007949 F0 | db 0F0h ; ð |
| 8 | .data:10007931 54 | db 54h ; T | 33 | .data:1000794A 69 | db 69h ; i |
| 9 | .data:10007932 FD | db 0FDh ; ý | 34 | .data:1000794B EE | db 0EEh ; ï |
| 10 | .data:10007933 F2 | db 0F2h ; ò | 35 | .data:1000794C 8F | db 8Fh ; ŠŠŠ |
| 11 | .data:10007934 43 | db 43h ; C | 36 | .data:1000794D 1C | db 1Ch |
| 12 | .data:10007935 C0 | db 0C0h ; À | 37 | .data:1000794E 25 | db 25h ; % |
| 13 | .data:10007936 F9 | db 0F9h ; ù | 38 | .data:1000794F FA | db 0FAh ; ú |
| 14 | .data:10007937 3E | db 3Eh ; > | 39 | .data:10007950 AB | db 0ABh ; « |
| 15 | .data:10007938 9F | db 9Fh ; Ÿ | 40 | .data:10007951 08 | db 8 |
| 16 | .data:10007939 EC | db 0ECh ; ì | 41 | .data:10007952 A1 | db 0A1h ; ; |
| 17 | .data:1000793A B5 | db 0B5h ; µ | 42 | .data:10007953 C6 | db 0C6h ; È |
| 18 | .data:1000793B EB | db 0EBh ; ë | 43 | .data:10007954 87 | db 87h ; ‡ |
| 19 | .data:1000793C F0 | db 0F0h ; ð | 44 | .data:10007955 B4 | db 0B4h ; ´ |
| 20 | .data:1000793D 4A | db 4Ah ; J | 45 | .data:10007956 DD | db 0DDh ; Ý |
| 21 | .data:1000793E BB | db 0BBh ; » | 46 | .data:10007957 52 | db 52h ; R |
| 22 | .data:1000793F D8 | db 0D8h ; Ø | 47 | .data:10007958 23 | db 23h ; # |
| 23 | .data:10007940 31 | db 31h ; l | 48 | .data:10007959 20 | db 20h |
| 24 | .data:10007941 16 | db 16h | 49 | .data:1000795A D9 | db 0D9h ; Ù |
| 25 | .data:10007942 EB | db 0EBh ; ë | 50 | .data:1000795B 9E | db 9Eh ; ž |

(c) Obfuscated Code in .data segment (MD5 hash = 6WbENDkcC750euPGqApQ)

Figure C.11: Code obfuscation in Vundo Trojan. (a) and (b) have the same code in .text section whereas (c) obfuscated that in its .data section

Appendix C.2. Simda Backdoor

We also found that most of the malware from this family is getting matched with consensus sequence where they are calling the `GetCurrentThreadId` function which is one of the most important prerequisites for a backdoor (see Figure C.12), and thus, we found this function in the report by various sandboxes for previously found backdoors, e.g., JoeSandbox [JoeSandbox \(2023\)](#), Falcon Sandbox [CrowdStrike \(2018-2019\)](#), etc.

```

1  .text:00402862 53          push    ebx
2  .text:00402863 56          push    esi
3  .text:00402864 52          push    edx
4  .text:00402865 57          push    edi
5  .text:00402866 51          push    ecx
6  .text:00402867 8D 05 2C D0 40 00  lea    eax, dword_40D02C
7  .text:0040286D 50          push    eax
8  .text:0040286E FF 35 19 D3 40 00  push   dword_40D318+1
9  .text:00402874 6A 5F          push   5Fh
10 .text:00402876 8D 05 7B D1 40 00  lea    eax, dword_40D179+2
11 .text:0040287C 50          push    eax
12 .text:0040287D 6A 12          push   12h
13 .text:0040287F 81 2D 53 D4 40 00 36 1C 00 00  sub    dword_40D452+1, 1C36h
14 .text:00402889 57          push    edi
15 .text:0040288A 6A 00          push   0
16 .text:0040288C 6A 3A          push   3Ah
17 .text:0040288E 56          push    esi
18 .text:0040288F C7 05 BE D2 40 00 C5 00 00 00  mov    dword ptr unk_40D2BE, 0C5h
19 .text:00402899 8D 05 7E D2 40 00  lea    eax, unk_40D27E
20 .text:0040289F 50          push    eax
21 .text:004028A0 E8 5F F7 FF FF    call   sub_402004
22 .text:004028A5 01 05 1B D4 40 00  add    dword ptr unk_40D41B, eax
23 .text:004028AB 6A 00          push   0 ; lpName
24 .text:004028AD 6A 00          push   0 ; bInitialState
25 .text:004028AF 6A 01          push   1 ; bManualReset
26 .text:004028B1 6A 00          push   0 ; lpEventAttributes
27 .text:004028B3 FF 15 C8 B0 40 00  call   ds:CreateEventW
28 .text:004028B9 29 05 6D D1 40 00  sub    off_40D16A+3, eax
29 .text:004028BF FF 15 98 B0 40 00  call   ds:GetCurrentThreadId
30 .text:004028C5 A3 F9 D3 40 00    mov    dword_40D3F6+3, eax
31 .text:004028CA 33 FF          xor    edi, edi
32 .text:004028CC 29 3D CB D2 40 00  sub    dword_40D2CA+1, edi
33 .text:004028D2 8B DF          mov    ebx, edi
34 .text:004028D4 FF 05 CA D2 40 00  inc    dword_40D2CA
35 .text:004028DA 8B FB          mov    edi, ebx
36 .text:004028DC 4F          dec    edi

```

Figure C.12: `GetCurrentThreadId` function call by Simda Backdoor matched with consensus sequence

Appendix C.3. Kelihos_ver1 Backdoor

Figure C.13 is one of the examples where our consensus sequence got matched with byte sequence that might be related to a malicious function. But here an important observation is – the order of the suspicious calls is different in different samples. All of them are checking for admin privileges and reboot requirement. While the malware in Figures C.13a and C.13b declares IsNTAdmin before RebootCheckInstall, malware in Figure C.13c does not. But still, they get detected by MALIGN.

```

1  .text:0048C010 49 73 4E 54 41 64 6D 69 6E 00  db 'IsNTAdmin',0
2  .text:0048C01A 00 00 word_48C01A dw 0 ; DATA XREF: .text:0048AF18(CANo
3  .text:0048C01C 52 65 62 6F 6F 74 43 68 65 63+ db 'RebootCheckOnInstall',0
4  .text:0048C031 00 00 word_48C031 dw 0 ; DATA XREF: .text:0048AF1C(CANo
5  .text:0048C033 44 65 6C 4E 6F 64 65 52 75 6E+ db 'DelNodeRunDLL32',0
6  .text:0048C043 00 00 word_48C043 dw 0 ; DATA XREF: .text:0048AF20(CANo
7  .text:0048C045 44 6F 49 6E 66 49 6E 73 74 61+ db 'DoInfInstall',0
8  .text:0048C052 00 00 word_48C052 dw 0 ; DATA XREF: .text:0048AF24(CANo

```

(a) First checks for admin privilege, then calls suspicious functions from IEAdvpack.dll and deletes file (0YJRabHQ1reDxN3yjUCd)

```

1  .text:00489819 49 73 4E 54 41 64 6D 69 6E 00  db 'IsNTAdmin',0
2  .text:00489823 00 00 word_489823 dw 0 ; DATA XREF: .text:00488A34(CANo
3  .text:00489825 52 65 62 6F 6F 74 43 68 65 63+ db 'RebootCheckOnInstall',0
4  .text:0048983A 00 00 word_48983A dw 0 ; DATA XREF: .text:00488A38(CANo
5  .text:0048983C 52 65 67 53 61 76 65 52 65 73+ db 'RegSaveRestoreOnINF',0
6  .text:00489850 00 00 word_489850 dw 0 ; DATA XREF: .text:00488A3C(CANo
7  .text:00489852 55 73 65 72 55 6E 49 6E 73 74+ db 'UserUnInstStubWrapper',0
8  .text:00489868 00 00 word_489868 dw 0 ; DATA XREF: .text:00488A40(CANo

```

(b) First checks for admin privilege, then calls suspicious functions from IEAdvpack.dll (7cx4QdBWg9wMa2pvOLuo)

```

1  .text:0048C920 52 75 6E 53 65 74 75 70 43 6F+ db 'RunSetupCommand',0
2  .text:0048C930 00 00 word_48C930 dw 0 ; DATA XREF: .text:0048BBBC(CANo
3  .text:0048C932 52 65 62 6F 6F 74 43 68 65 63+ db 'RebootCheckOnInstall',0
4  .text:0048C947 00 00 word_48C947 dw 0 ; DATA XREF: .text:0048BBC0(CANo
5  .text:0048C949 47 65 74 56 65 72 73 69 6F 6E+ db 'GetVersionFromFileEx',0
6  .text:0048C95E 00 00 word_48C95E dw 0 ; DATA XREF: .text:0048BBC4(CANo
7  .text:0048C960 49 73 4E 54 41 64 6D 69 6E 00  db 'IsNTAdmin',0
8  .text:0048C96A 00 00 word_48C96A dw 0 ; DATA XREF: .text:0048BBC8(CANo

```

(c) First calls suspicious functions from IEAdvpack.dll, then checks for admin privilege (d5ki60fcbqeh3SvZzpoB)

Figure C.13: Suspicious Windows function calls by Kelihos (version 1) got detected by MALIGN

Appendix D. Robustness

Appendix D.1. Plausible Techniques to Evade MALIGN

To evade our model, some possible attacks and the robustness of our model against them are discussed below:

- *Including pieces of other malware to confuse family detection:* The inclusion of pieces from other malware will be detected but code-pieces of the original family will also be detected at the same time, and consequently, the score for the original family should be higher since it contains more code-pieces than the other family. However, if an attacker can include enough code-segments from other families that can outnumber the score for the real family, MALIGN might predict a wrong family. One defense against this attack can be to incorporate monotonic classifier [İncir Romeo et al. \(2018\)](#), or non-negative network [Fleshman et al. \(2018a\)](#) with MALIGN.
- *Code Randomization:* Attackers can try to replace instructions with semantically similar ones to evade MALIGN [Song et al. \(2020\)](#). However, the attacker will have to change a lot of instructions so that it does not get aligned with enough consensus sequences which is not a trivial task, not impossible at the same time. To defend against such attacks, we can generate artificial adversarial malware using code randomization and train MALIGN using them to capture the signature for such code randomizations.
- *Register Reassignment:* An attacker can add multiple instructions that reassign registers and create an adversarial malware that has different sequences than our signature [Lucas et al. \(2021\)](#). One way to defend against this attack with MALIGN can be – changes in the alignment algorithm (or apply heuristic) so that it becomes flexible against register names and instructions.
- *Instruction Reordering:* Attackers can try changing the order of instructions without harming the functionality of malware. MALIGN is robust to such attack to some extent, and we discovered that in one of our consensus sequences (see [Figure C.13](#)). However, if the order is jumbled to an extreme, possibly through the use of jump instructions, it might get evaded.

Appendix D.2. Direct Attack on MALIGN

Besides the above mentioned approaches, an attacker can try generating adversarial malware specifically for MALIGN in a white-box setting. Since MALIGN is hard to invert and is non-differentiable, the attacker cannot compute gradient or apply reverse engineering unlike other end-to-end deep learning models. They will have to replace the feature mapping function, or especially the MSA tool with the best approximated model [Petti et al. \(2021\)](#) to create an adversarial sample. But replacing an MSA with approximated DNN is another challenging task. Moreover, when the attacker has to preserve the semantics, creating such an approximated model becomes even harder.

Appendix E. Consensus Sequence Analysis

We analyzed the conserved sequences to estimate the number of informative code blocks for each malware family. Table E.14 (in Appendix) represents the number of consensus sequences, i.e., conserved blocks and the number of informative code blocks for each family in the Kaggle Microsoft dataset. We term a code block ‘informative’ if the value of the corresponding weight in our regression model is positive. The rationale behind this is that - the higher the weight of the consensus sequence, the higher impact it has on the classification.

We can observe from the table that, the number of consensus sequences found by MALIGN is proportional to the number of samples in a malware family. However, the percentage of the number of informative consensus sequences varies across malware families. The percentage values indicate that large fractions of blocks identified through the sequence alignment process are useful for the subsequent classification task.

| Family Name | Number of Consensus Sequence | Number of Informative Consensus Sequence | Percentage of Informative Consensus Sequence |
|----------------|------------------------------|--|--|
| Ramnit | 962129 | 177905 | 18.49% |
| Kelihos_ver3 | 331432 | 105223 | 31.75% |
| Vundo | 27210 | 17601 | 64.69% |
| Simda | 3098 | 1194 | 38.54% |
| Tracur | 37967 | 20548 | 54.12% |
| Kelihos_ver1 | 27459 | 13467 | 49.04% |
| Obfuscator.ACY | 94172 | 42863 | 45.51% |
| Gatak | 275984 | 96554 | 34.99% |

Table E.14: Number of Consensus Sequence in Malware Families